Enterprise Control Assessment for the Mitigation of Renewable Energy by Demand Side Management

by

Bo Jiang

Submitted to the Department of Mechanical Engineering
in partial fulfillment of the requirements for the degree of

Master of Science in Mechanical Engineering

at the

MASSACHUSETTS INSTITUTE OF TECHNOLOGY

June 2015

Author ..... Signature redacted
Department of Mechanical Engineering
May 19, 2015

Certified by.... Signature redacted .....
Kamal Youcef-Toumi
Professor
Thesis Supervisor

Signature redacted

Accepted by .....
David E. Hardt
Chairman, Department Committee on Graduate Theses

Enterprise Control Assessment for the Mitigation of Renewable Energy by Demand Side Management

by

Bo Jiang

Submitted to the Department of Mechanical Engineering
on May 19, 2015, in partial fulfillment of the
requirements for the degree of
Master of Science in Mechanical Engineering

Abstract

The traditional power grid paradigm of centralized and actively controlled power generation facilities serving distributed and passively controlled electrical loads is challenged by the requirements for decarbonization, enhanced reliability and transportation electrification. The power grid will undergo technical, economic and regulatory changes and motivates new control and automation technologies and incentivized Demand Side Management (DSM) to accommodate the intermittent and distributed nature of renewable energy. The first phase of this thesis is an extensive review of existing renewable energy integration study methodologies and their limitations. On the other hand, a newly developed holistic enterprise control assessment method manages the diversity of control solutions and many competing objectives, is case independent, addresses both physical nature as well as enterprise control processes, and is validated by a set of numerical simulations. Another major omission in the majority of integration studies is the demand side resources.

Demand Side Management with its ability to allow customers to adjust electricity consumption in response to market signals has often been recognized as an efficient way to mitigate the variable effects of renewable energy as well as to increase system efficiency and reduce system costs. Dispite the recongnized importance of DSM, the academic & industrial literature have taken divergent approaches to DSM implementation. While the popular approach among academia adopts a social welfare maximization formulation, the industrial practice compensates customers according to their load reduction from a predefined electricity consumption baseline that would have occurred without DSM.

This thesis then rigorously compares the two different DSM approaches in a day-ahead electricity wholesale market analytically and numerically using the same system configuration and mathematical formalism. The comparison of the two models showed that a proper reconciliation of the two models might make them mitigate the stochastic netload in fundamentally the same way given an industrial baseline equal to the dispatchable demand forecast in the social welfare model, which is rarely met in practice. While the social welfare model uses a stochastic net load composed of

two terms, the industrial DSM model uses a stochastic net load composed of three terms including the additional baseline term. DSM participants have the incentives to manipulate the baseline in order to receive greater financial compensation, taking advantage of greater awareness of their facilities than the regulatory agencies charged with estimating the baseline. In a day-ahead wholesale market, the artificially inflated baseline forecast used in the industrial formalism is shown to result in higher and costlier dispatchable resources scheduling and unachievable social welfare compared to the academic method.

This thesis proceeds to compare the two DSM approaches and quantifies the technical impact of industrial baseline errors in subsequent layers of control using an enterprise control methodology. The baseline inflation errors in a day-ahead market have to be corrected in the downstream enterprise control activities at faster time scales, increasing the control efforts and reserve requirements in the real-time market dispatch and regulation service respectively. The adoption of enterprise control simulator added with a dispatchable demand module enables the simultaneous study of day-ahead and real-time market, regulation service and power flow analysis. The day-ahead wholesale market adopts a unit commitment problem and the real-time wholesale market adopts an economic dispatch (ED) problem on the timescale of minutes. While baseline error is absent in the social welfare model, the industrial model is simulated with different baseline levels, assuming the baseline inflation has the same effects in the day-ahead and real-time market. The resulting implications of baseline errors on power grid imbalances and regulating reserve requirements are tracked. It is concluded that with the same regulating service, the introduction of baseline error leads to additional system imbalance compared to the social welfare model results, and the imbalance amplifies itself as the baseline error increases. As a result, more regulating reserves are required to achieve the same satisfactory system performance with higher baseline error.

In summary, the industrial DSM baseline inflation brings about higher and costlier dispatch in day-ahead wholesale market and higher reserve requirements in subsequent control layers, namely the real-time market regulating service.

Thesis Supervisor: Kamal Youcef-Toumi
Title: Professor

Acknowledgments

First and foremost I wish to thank my advisor, Professor Kamal Youcef-Tomi for supporting and encouraging me throughout my thesis with not only his constructive research advice but also his caring and patience. He provided an excellent research atmosphere and set a model for me to follow.

My sincere thank you also goes to my co-advisor, Professor Amro M. Farid, for continuously guiding me with his knowledge and efforts. I cannot remember how many late evenings he had to discuss my work from Abu Dhabi to accommodate our 8-hour time difference.

I am lucky to have a friendly group of people at MRL. I would especially like to thank Dr. Aramazd Muzhikyan from LINES for teaching me every coding tricks.

I take this opportunity to express my gratitude to MIT Energy Initiative and Ferrovial for awarding me MIT Energy Initiative Ferrovial Fellowship for the academic year 2013/2014, MIT Department of Mechanical Engineering for awarding me Sontheimer Travel Award Spring 2015. Only with their help can I finish this work.

I am blessed with my most wonderful parents. My moms unconditional support and my dads sense of humor travel through oceans on various chatting software I force them to use. I will always be grateful for their companion, and sharing all the happiness in my life.

THIS PAGE INTENTIONALLY LEFT BLANK

Contents

THIS PAGE INTENTIONALLY LEFT BLANK

List of Figures

THIS PAGE INTENTIONALLY LEFT BLANK

List of Tables

THIS PAGE INTENTIONALLY LEFT BLANK

Nomenclature

GC	subscript for dispatchable (controllable) generators (e.g. thermal plants)
GS	subscript for stochastic generators (e.g. wind, solar photo-voltaic)
DC	subscript for dispatchable (controllable) demand units (i.e. participating in DSM)
DS	subscript for stochastic demand units (i.e. conventional load)
i	index of dispatchable generators
j	index of dispatchable demand unit
l	index of stochastic generators
k	index of stochastic demand unit
b	index of buses
h	index of lines
T	index of unit commitment time intervals
t	index of regulation time points
N_{GC}	Number of dispatchable generators
N_{DC}	Number of dispatchable demand units
N_{GS}	Number of stochastic generators

N_{DS} Number of stochastic demand units

N_B Number of buses

N_T Number of unit commitment time intervals

N_t Number of economic dispatch time points

T_{ED} real-time market time step

$\mathcal{W}$ social welfare

$\mathcal{U}_{DCj}$ demand utility of the jth dispatchable demand unit

$\mathcal{S}_{DCj}$ startup utility of the jth dispatchable demand unit

$\mathcal{D}_{DCj}$ shutdown utility of the jth dispatchable demand unit

$\mathcal{R}_{DCjT}$ running utility of the jth dispatchable demand unit in the Tth unit commitment time interval

$\mathcal{C}_{GCi}$ cost of the ith dispatchable generator

$\mathcal{S}_{GCi}$ startup cost of the ith dispatchable generator

$\mathcal{D}_{GCi}$ shutdown cost of the ith dispatchable generator

$\mathcal{R}_{GCiT}$ running cost of the ith dispatchable generator in the Tth unit commitment time interval

$\mathcal{C}_{DCj}$ cost of the jth virtual generator

$\mathbb{S}_{DCj}$ startup cost of the jth virtual generator

$\mathbb{D}_{DCj}$ shutdown cost of the jth virtual generator

$\mathbb{R}_{DCjT}$ running cost of the jth virtual generator in the Tth unit commitment time interval

$\Delta\mathcal{W}_t$ incremental social welfare at time t

$\Delta\mathcal{U}_{DCjt}$ incremental utility of the jth dispatchable demand unit at time t

$\Delta\mathcal{C}_{GCit}$ incremental cost of the ith dispatchable generator at time t

$\Delta\mathcal{C}_{DCjt}$ incremental cost of the jth virtual generator at time t

A_{DCj} quadratic utility function coefficient of the jth dispatchable demand unit

B_{DCj} linear utility function coefficient of the jth dispatchable demand unit

ζ_{DCj} utility function constant of the jth dispatchable demand unit

A_{GCi} quadratic cost function coefficient of the ith dispatchable generator

B_{GCi} linear cost function coefficient of the ith dispatchable generator

ζ_{GCj} cost function constant of the ith dispatchable generator

$\mathbb{A}_{DCj}$ quadratic cost function coefficient of the jth virtual generation

$\mathbb{B}_{DCj}$ linear cost function coefficient of the jth virtual generation

ξ_j cost function constant of the jth virtual generation

w_{DCjT} binary variable for the state of the ith dispatchable demand unit in the Tth unit commitment time interval

u_{DCjT} binary variable for the startup state of the jth dispatchable demand unit in the Tth unit commitment time interval

v_{DCjT} binary variable for the shutdown state of the jth dispatchable demand unit in the Tth unit commitment time interval

w_{GCiT} binary variable for the state of the ith dispatchable generator in the Tth unit commitment time interval

u_{GCiT} binary variable for the startup state of the ith dispatchable generator in the Tth unit commitment time interval

v_{GCiT} binary variable for the shutdown state of the ith generator in the Tth unit commitment time interval

ω_{DCjT} binary variable for the state of the jth virtual generation in the Tth unit commitment time interval

μ_{DCjT} binary variable for the startup state of the jth virtual generation at the beginning of the Tth unit commitment time interval

ν_{DCjT} binary variable for the shutdown state of the jth virtual generation at the beginning of the Tth unit commitment time interval

P_{DCjT} dispatched power consumption at the jth dispatchable demand unit in the Tth unit commitment time interval

P_{GCiT} dispatched power generation at the ith dispachable generator in the Tth unit commitment time interval

$\hat{P}_{DCjT}$ forecasted power consumption of the jth dispatchable demand unit in the Tth unit commitment time interval

$\tilde{P}_{DCjT}$ baseline power consumption of the jth dispatchable demand unit in the Tth unit commitment time interval

$\hat{P}_{GSkT}$ forecasted power generation at the kth stochastic generator in the Tth unit commitment time interval

$\hat{P}_{DSlT}$ forecasted power consumption of the lth stochastic demand unit in the Tth unit commitment time interval

P_{DCjt} dispatched power consumption at the jth dispatchable demand unit at time t

ΔP_{DCjt} incremental power consumption at the jth dispatchable demand unit at time t

P_{GCit} dispatched power generation at the ith dispachable generator at time t

ΔP_{GCit} incremental power generation at the ith dispachable generator at time t

$\tilde{P}_{DCjt} - P_{DCjt}$ dispatched power generation at the jth virtual generator at time t

F_{ht} power flow level of line h at time t

M_{bi} correspondence matrix of dispatchable generator i to bus b

M_{bj} correspondence matrix of dispatchable demand unit j to bus b

ΔP_{bt} dispatchable generation increments on bus b at time t

ΔD_{bt} dispatchable demand increments on bus b at time t

$\Delta \hat{D}_{bt}$ stochastic demand forecast increments on bus b at time t

γ_{bt} incremental transmission loss factor of bus b at time t

a_{hbt} bus b generation shift distribution factor to line h

$\underline{P_{GCi}}$ min. capacity of the ith dispatchable generator

$\underline{P_{DCj}}$ min. capacity of the jth dispatchable demand unit

$\underline{R_{GCi}}$ min. ramping capability of the ith dispatchable generator

$\underline{R_{DCj}}$ min. ramping capability of the jth dispatchable demand unit

$\overline{P_{GCi}}$ max. capacity of the ith dispatchable generator

$\overline{P_{DCj}}$ max. capacity of the jth dispatchable demand unit

$\overline{R_{GCi}}$ max. ramping capability of the ith dispatchable generator

$\overline{R_{DCj}}$ max. ramping capability of the jth dispatchable demand unit

$\underline{\tilde{P}_{DCj} - P_{DCj}}$ min. capacity of the jth virtual generator

$\overline{\tilde{P}_{DCj} - P_{DCj}}$ max. capacity of the jth virtual generator

$\overline{F_h}$ flow limit of line h

THIS PAGE INTENTIONALLY LEFT BLANK

Chapter 1

Introduction

1.1 Research Motivation

Traditional power system are often built on the basis of centralized and actively controlled power generation facilities serving distributed and passively controlled electrical loads to achieve maximum grid reliability regardless of production costs. However, this paradigm is challenged by the requirements for decarbonization, enhanced reliability and transportation electrification. [1] The power grid will undergo technical, economic and regulatory changes and motivates new control and automation technologies and incentivized DSM to accommodate the intermittent and distributed nature of renewable energy. [1]

An extensive academic and industrial literature has been developed to determine the technical and economic feasibility of integrating a certain amount of variable energy resources [4, 5, 6, 7, 8, 9, 10, 11]. Piece-meal integration and a lack of coordinated assessment could result in misunderstanding of system reliability and over-costly solutions. The first stage of this thesis is a review of the existing renewable energy integration study methodologies and an analysis of their limitations. In contrast to the extensive integration studies previous to it, a newly developed holistic enterprise control assessment method manages the diversity of control solutions and many competing objectives. This assessment method for variable energy resource induced power system imbalances was developed based on the concept of enterprise control [12, 13].

This holistic assessment method is case independent, addresses both physical grid as well as enterprise control process, and is validated by a set of numerical simulations [14, 15, 16] The simulator consists within a single package most of the balancing operation functionality found in traditional power systems.

Demand Side Management (DSM) with its ability to allow customers to adjust electricity consumption in response to market signals has often been recognized as an efficient way to mitigate the variable effects of renewable generation[17, 18, 19]. The fast fluctuations in renewable energy generation require high ramping capability which must be balanced by dispatchable energy resources. Additionally, a sudden loss of renewable generation can threaten grid reliability in the absence of adequate generation reserves. DSM has also been advocated for its ability to increase system efficiency and reduce system costs by peak load shaping and shifting[20, 21]. By enabling peak load shaving, DSM provides additional dispatchable resources[22, 23], which can potential offset imbalances caused by renewable energy and reduce the need for more expensive generators with high ramping capability. It also increases the bulk electric system reliability by disengaging some loads at challenging periods. Meanwhile, DSM increases the utilization of generating capacities that would have been otherwise idle during off-peak hours, thus reducing the real cost of renewable integration[24]. The electricity supply side, load-reducing customers and non-load-reducing customers all benefit economically from load reductions[25, 26].

Despite its recognized importance[27, 28, 29], the industrial and academic literature seem to have taken divergent approaches to DSM implementation. A common approach among academic researchers is to maximize social welfare defined as the net benefits from electricity consumption and generation based on the utility of dispatchable demand [30, 31, 32, 33]. In the meantime, the industrial trend has been to introduce "virtual generators" in which customers are compensated for load reductions from baseline electricity consumption [34, 35, 36, 37, 38, 39, 40]. Such a baseline is defined as the counterfactual electricity consumption that would have occurred without DSM and is estimated from historical data from the prior year [41, 42, 43]. Thus, dispatchable demand reductions are also treated as "virtual generators".

The industrial baselines easily involve errors and are most likely to be different from the load forecast. Firstly, the methods of determining the load forecast and industrial baseline are fundamentally different. While the latter is calculated a day in advance based upon sophisticated methods [44], the formulae for baseline are much more basic and determined months in advance [45, 46, 47, 48, 49]. Indeed, it is conceivable that a baseline is set and then the demand side participant makes (static) long-term energy efficiency improvements and then is compensated for the now guaranteed "load-reduction". As several authors note, the baseline itself is subject to manipulation because DSM participants have greater awareness of their facilities than the regulatory agencies charged with estimating the baseline [50, 51]. Unfortunately baselines are subject to manipulations and false load reductions can be created for more compensations[50, 51]. While the differences between the two methods have often been a part of policy discussions, they have not been rigorously studied. This thesis first aims to rigorously compare these two different approaches in a day-ahead wholesale market context using the same system configuration and mathematical formalism.

During research process detailed in Chapter 3, it is demonstrated that while the net load in the academic DSM is composed of two terms, the net load in the industrial DSM is composed of three with an additional baseline term and, therefore, introduces additional forecast errors. The work showed the equivalence of the two methods provided that 1) the utility function of dispatchable demand and the cost function of virtual generation are properly reconciled and 2) the industrial baseline is the same as the load forecast. However, the accuracy of baseline forecast is not likely achievable, since the load forecast is calculated a day in advance based upon sophisticated methods [44], while the baseline calculation involves much more basic formulae and is determined months in advance [45, 47]. Indeed, the customers have an implicit incentive to surreptitiously inflate the administrative baseline for greater compensation, taking advantage of greater awareness of their facilities than the regulatory agencies charged with estimating the baseline [50, 51]. In Chapter 3, successful baseline manipulation is shown to result in higher levels of day-ahead dispatchable

resources scheduling and higher costs in the unit commitment problem. As a result, this baseline error have to be corrected in downstream enterprise control activities at faster time scales, likely requiring greater control effort and higher reserve amounts. This thesis then proceed to compare the two approaches of DSM and seek to quantify the technical impact of baseline error in subsequent control layers using an enterprise control simulator added with a dispatchable demand module. Such assessment is enabled by the recently developed enterprise control assessment method described in Chapter 2.

1.2 Research Objectives and Questions

To resolve the gap between academic and industrial literature gap on the topic of DSM, the thesis has the following objective. This objective is broken down into several questions.

Research Objective: To compare the academic social welfare and industrial load reductions DSM methods, and study the effects of baseline errors in the context of enterprise control.

Research Question 1: How can an enterprise control assessment method incorporate physical grid properties and all important balancing control functionality?

Research Question 2: How are the academic social welfare and industrial load reductions models different from each other?

Research Question 3: What is the economic effect of industrial baseline error in a day-ahead wholesale market?

Research Question 4: What is the technical effect of industrial baseline in real-time market and regulation service?

1.3 Research Approach

This thesis is approached in four phases:

Research Identification: First,the research problem of comparing academic and

industrial DSM in the context of enterprise control is identified by an analysis of the literature.

Analytical Modeling & Comparison: Next, the academic social welfare and industrial load reductions methods are mathematically modeled and reconciled. The equivalence conditions of the two models are determined through Lagrangian optimization equations.

Numerical Case Studies for a Day-Ahead Wholesale Market: The methods are then numerically compared in the context of a day-ahead wholesale market using case studies implemented with MATLAB interfaced with GAMS.

Numerical Case Studies with Enterprise Control Assessment: The comparison is then extended to subsequent control layers in the context of holistic assessment methods. The case study is implemented with an enterprise control simulator added with a dispatchable demand module.

1.4 Research Scope

A few remarks are made to define the scope of this thesis:

Wholesale Market: The comparison of the two DSM methods are restricted to an electricity wholesale market. Electricity markets are classified as wholesale or retail markets. Wholesale markets manage generation to transmission, while retail market starts from step-down transformers and distributes electricity to customers on a flat-rate.[52] The procurement and dispatch decision from TJE wholesale market is the result of different parties bidding on various time-scales [53] and therefore have variable electricity price. Wholesale markets are further classified into long-term capacity market, the short-term energy market, and the operating reserve market.

Enterprise Control Assessment: This thesis compares the two DSM approaches and quantifies the technical and economic impact of industrial baseline errors on

various timescales using an enterprise control methodology. The adopted enterprise control simulator encompasses three interconnected layers: a resource scheduling layer composed of a security-constrained unit commitment (SCUC), a balancing layer composed of a security-constrained economic dispatch (SCED), and a regulation layer.

1.5 Novelty of Research Contributions

The novel contributions of this work are:

- Summaries the existing literature on renewable energy integration studies.
- Identifies the gap of academic and industrial literature on DSM implementation.
- Develops and reconciles social welfare and industrial load reductions DSM models using the same system configuration and mathematical formalism.
- Proves the equivalence conditions of the two models through theoretical analysis and numerical case study.
- Demonstrates rigorously the technical and economic effects of industrial DSM baseline inflation in day-ahead wholesale market, real-time market, and regulating serves using an enterprise control assessment method

1.6 Organization of Thesis

This research is explained over the remaining of four chapters.

- Chapter 2 motivates the need for the holistic assessment method of renewable energy integration with the ability to manage the diversity of control solutions. A framework for power grid enterprise control assessment is described and contrasted to existing variable energy resource integration studies. Two different approaches to DSM are introduced and the need for comparison is argued.

- Chapter 3 rigorously compares the social welfare and the industrial load reduction approaches, proves the equivalence conditions of the two models analytically and numerically, and numerically studies the effects of an erroneous industrial baseline in a day-ahead wholesale market context

- Chapter 4 compares the social welfare and industrial DSM methods and quantifies the technical impact of baseline error in subsequent control layers, namely the real-time market control layer and regulation service layer, using an enterprise control assessment method.

- Chapter 5 brings the thesis to a close with conclusions about the model difference between the social welfare and industrial load reduction DSM methods and the technical and economic effects of industrial baseline inflation.

THIS PAGE INTENTIONALLY LEFT BLANK

Chapter 2

The Need for Holistic Power Grid Enterprise Control Assessment & Demand Side Management

2.1 The Need for Holistic Power Grid Enterprise Control Assessment

In this subsection, current renewable energy integration study methods trending and the associated limitations are reviewed and analyzed. A newly proposed holistic power grid enterprise control assessment method is then summarized, and its advantages are described. The need for DSM in the context of enterprise control is argued, and two different approaches of DSM in academic and industrial literature are summarized and contrasted.

2.1.1 Limitations of Existing Assessment Methods

The requirements for decarbonization, enhanced reliability and transportation electrification motivates new control and automation technologies and consumer participation. While piece-meal assessment cannot capture all technical challenges, uncoordinated assessments result in costly overbuilt solutions. [1] Extensive studies

			Physical Layer				Cyber-Layer (Control)			Assessment Method for Power System Objectives						
										Balancing Operation						
	Acronym	Publication Year	Dispatchable Generation	Variable Generation	Traditional Load	Demand Side Resources	Unit Commitment	Economic Dispatch	Regulation	Load Following (Secondary) Reserves	Ramping Reserves	Regulation (Primary) Reserves	Line Congestion Management	Voltage Management	Operating Cost	Investment Cost
1	CA-MA-WIS	2005	✓	Wind	✓	--	N/A -- Stats Only			--	--	--	--	--	--	--
2	CA-ON-WIS	2006	✓	Wind	✓	--	N/A -- Stats Only			Stat-B-VAR 5min	--	Stat-B-VAR 1min	--	--	--	--
3	EU-AI-REIS	2007	✓	All	✓	--	Gen: 1h	Gen: 1h	Gen: 1h	Stoch-WLF 5min	--	Stat-D2-WLF	--	--	UCED	--
4	EU-IB-WIS	2006	✓	Wind	✓	--	N/A -- Dynamics Only			--	--	--	--	--	--	--
5	EU-DE-WIS	2005	✓	All	✓	--	N/A -- Stats Only			Stat-D2-WLF 15min	--	--	PFA, N-1CA	DVSM	--	Physical: Lines, Control:
6	EU-DE-REIS	2010	✓	All	✓	Storage & DSM	G&D: 1h	G&D: 1h	--	Utilized	Residual Load Duration	--	PFA	SVSM	UCED	Physical: Lines
7	EU-NL-WIS	2009	✓	Wind	✓	Storage	Gen: 1h	Gen: 1h	Gen: 1s	--	--	--	--	--	UCED	--
8	EU-SE-WIS	2005	✓	All	✓	--	N/A -- Stats Only			Stat-B-WLF 1h	--	Stat-B-WLF 15min	--	--	--	--
9	EU-REIS	2012	✓	All	✓	Storage & DSM	G&D: 1h	G&D: 1h	--	Utilized	Residual Load Duration	--	--	--	UCED	Physical: Generation
10	EU-WIS	2010	✓	All	✓	--	Gen: 1h	Gen: 1h	Gen: 1s	--	--	--	PFA, N-1CA	DVSM	UCED	Physical: Lines
11	EU-TW-WIS	2009	✓	Wind	✓	--	Gen: 1h	Gen: 1h	--	--	--	--	PFA	--	UCED	--
12	EU-UK-WIS	2007	✓	Wind	✓	--	N/A -- Stats Only			Stat-B-WLF 30min	--	--	--	--	--	--
13	EU-WI-WIS	2005	✓	Wind	✓	--	--	Gen: 5min	Gen: 1s	Utilized	--	Utilized	UCED	--	UCED	--
14	US-AV-WIS	2007	✓	Wind	✓	Storage	Gen: 1h	Gen: 1h	--	Stat-B-VAR 10min	--	Stat-B-VAR 10min	--	--	UCED	--
15	US-AZ-SIS	2012	✓	Solar	✓	--	N/A -- Stats Only			Stat-D1-WLF 10min	--	--	--	--	Stat	--
16	US-CA-REIS	2010	✓	All	✓	--	Gen: 1h	Gen: 5min	Gen: 1s	Stoch 5min	Stoch 1min	Stoch 1min	--	--	UCED	--
17	US-E-WIS	2010	✓	Wind	✓	--	Gen: 1h	Gen: 1h	--	Stat-D1-WLF Minutes	--	--	--	--	UCED	--
18	US-ERC-REIS	2008	✓	All	✓	--	Gen: 1h	Gen: 1h	--	--	--	Stat-B/ D1-WLF	--	--	UCED	--
19	US-HA-WIS	2011	✓	All	✓	--	Gen: 1h	Gen: 1h	Gen: 1s	Stat-D1 10min	--	Stat-D1 1s	--	--	UCED	--
20	US-ID-SIS	2014	✓	Solar	✓	--	--	Gen: 1h	--	Stat-B 5min	--	--	--	--	UCED	--
21	US-MN-WIS	2006	✓	Wind	✓	--	Gen: 1h	Gen: 1h	--	Stat-B-VAR Minutes	--	Stat-B-Var	PFA	--	UCED	--
22	US-NE-WIS	2010	✓	Wind	✓	--	Gen: 1h	Gen: 10min	--	Stat-D1 10min	--	Stat-D1 10min	--	--	UCED	--
23	US-NEng-WIS	2010	✓	Wind	✓	--	Gen: 1h	Gen: 1h	--	Stat-B 10min	--	Stat-B 10min	--	--	--	--
24	US-NV-SIS	2011	✓	Solar	✓	--	Gen: 1h	Gen: 10min	Gen: 2-4s	Stat-B-VAR 10min	Stat-VAR-1min	Stat-B-VAR 1min	--	--	UCED	--
25	US-NY-WIS	2005	✓	Wind	✓	--	Gen: 1h	Gen: 1h	--	Stat-B-Var 5min	--	Stat-B-Var	--	DVSM	UCED	--
26	US-P-WIS	2010	✓	Wind	✓	--	Gen: 1h	Gen: 1h	Gen: 10min	Stat-B-VAR 1h	--	Stat-B-VAR 10min	--	--	UCED	--
27	US-PJM-REIS	2013	✓	All	✓	--	Gen: 1h	Gen: 1h	--	Stat-D1-VAR 10min	--	Stat-D1-VAR 10min	Trans. overlay	--	UCED	Physical: Lines
28	US-SPP-WIS	2010	✓	Wind	✓	--	Gen: 1h	Gen: 1h	--	Stat-B-WLF 10min	--	Stat-B-WLF	PFA, N-1CA	SVSM	UCED	--
29	US-W-WSIS	2010	✓	All	✓	--	Gen: 1h	Gen: 5min	Gen: 1min	Stat-D1-VAR	--	--	PFA	--	UCED	--
30	US-W-WSIS2	2013	✓	All	✓	--	Gen: 1h	Gen: 5min	Gen: 1min	Stat-D1-VAR	--	Stat-D1-WLF	PFA	--	UCED	--

Key: PFA -- Power Flow Analysis, N-1CA -- N-1 Contingency Analysis, DVSM - Dynamic Voltage Stability Model, Static Voltage Stability Model

Figure 2-1: An Analysis of Scope and Methods in Renewable Energy Integration Studies [1]

have been developed to determine the feasibility of integrating a certain amount of renewable energy. However,their overall contribution to holistic dynamic properties such as flexibility and voltage stability calls for further study. An extensive literature was reviewed and analyzed, and the study methods are summarized Figure 2-1 [54, 55, 56, 57, 58, 59, 60, 61, 62, 63, 64, 65, 66, 67, 68, 69, 70, 71, 72, 73, 74, 75, 76, 77, 78, 79, 80, 81, 82, 83] in terms of physical layer, control layer, and assessment method for power system objectives. Balancing operations and reserves determination are two of the central objectives of renewable energy integration studies. [1] Reserves are classified in Figure 2-1 on the basis of timescales. The following paragraphs argue the limitations of integration study trending from the aspects of physical grid, balancing operations, line congestion and voltage stability management, and economic assessments.

In regards to the physical layer, most studies have focused on variable resources, giving little attention to demand side resources [63, 59]. In general, the standard deviation of potential imbalances is calculated using the probability distribution of net-load forecast error. The load following and regulation reserve requirements are then defined to cover appropriate confidence intervals of the distribution based on the experience of power system operators [84, 85, 86], or to comply with existing standards such as North American Electric Reliability Corporation (NERC) balancing requirements [87, 88, 89, 90]. This trend has several inherent limitations. First of all, these studies give no consideration to operating procedures and control techniques and thus is unlikely a sufficient approach to determine reserve requiements and describe system reliability. Instead of applying Unit Commitment Economic Dispatch (UCED) models and validating results by simulation [91, 92], most studies [93, 94, 95, 96] assesses the need for required operating reserves based on statistical analysis of stochastic resources. As pointed out by Farid [1], the reliability of the power grid depends ont only on the magnitude and timescale of a disturbances but also the control functions that attenuate this disturbance. Those wind power integration studies that do use simulation usually do so for a particular study area[97] and sometimes do not differentiate between timescales [90, 98, 91]. The second limitation arises from using solely

renewable energy standard deviation [84, 98, 86] or forecast error [89, 99, 100, 101]. However, a true determination of non-event reserves is likely to depend on both distinct variables [102]. A third concern is the the usage and treatment of different power system timescales in the integration studies. [1] Load following and regulation reserves operate at different but overlapping timescales. Netload variability exists on all timescales, forecast error exist in day-ahead and intra-hour timescales. While load following reserves are relevant to day-ahead forecast errors and variability, the short-term effects of variability and forecast errors are mostly mitigated by regulation reserves. One study [90] distinguishes between three different timescales of power system imbalances: intra-hour variability, minute-by-minute variability and day-ahead forecast error. However, this division of impacts is not carefully addressed in a large number of studies [84, 88].

From the power system enterprise control view, most renewable energy integration studies use simulations based upon an integrated UCED model. Fewer studies add a model of regulation as a separate ancillary service. Another often cited concern is that these simulations should correspond to the existing operating reality on key factors such as time steps, market structure and physical constraints [103, 104, 94, 95, 96].

Some studies have also included line congestion and voltage management even though frequency balancing operations have been the focus of integration studies. Line congestion management are usually conducted with power flow and contingency analysis post to UCED simulations. Holttinen et al. suggest instead that these should analyses be integrated[94, 95]. More fundamentally line congestion and the stability of balancing operations are ultimately coupled[105, 106, 107] and should be integrated in simulation[104].

The economic assessment in most integration studies are often focused on operational costs through unit commitment and economic dispatch simulations in conjunction with statistical analysis. Few studies address the investment cost of voltage regulators [59] or ancillary service [108].

Despite the above-mentioned limitations, the integration studies as a collection establish a holistic understanding of the power grid, upon which an enterprise control

assessment method is developed.

2.1.2 A Framework for Holistic Power Grid Enterprise Control Assessment

A holistic power grid enterprise control assessment has been recently developed in Reference [1] to address the literature gap. From the aspect of involving power grid itself, this newly assessment method allows for an evolving mixture of generation and demand as dispatchable energy resources, an evolving mixture of generation and demand as variable energy resources, and the simultaneous study of transmission and distribution systems. [1] To address the grid behavior in the operation timescale, the method allows for the time domain simulation of the convolution of grid enterprise control functions and grid topology reconfiguration. The incorporation of physical grid and control functions allows the study of the holistic dynamic properties of dispatchability, flexibility, forecastability, stability, and resilience, and further the potential changes in enterprise grid control functions and technologies as impacts on these dynamic properties. [1] Finally, the method accounts for the consequent changes in operating cost and the required investment costs. [1]

Figure 2-2 provides a visualization of the enterprise control simulation [109, 13, 110, 111, 112]. On top of the physical grid, the control functions are implemented by three interconnected layers: a resource scheduling layer composed of a security-constrained unit commitment (SCUC), a balancing layer composed of a security-constrained economic dispatch (SCED), and a regulation layer. [1] Power flow analysis as a physical model of the power grid is integrated into the simulation and serves to recalibrate the SCUC, SCED and regulation simulations.

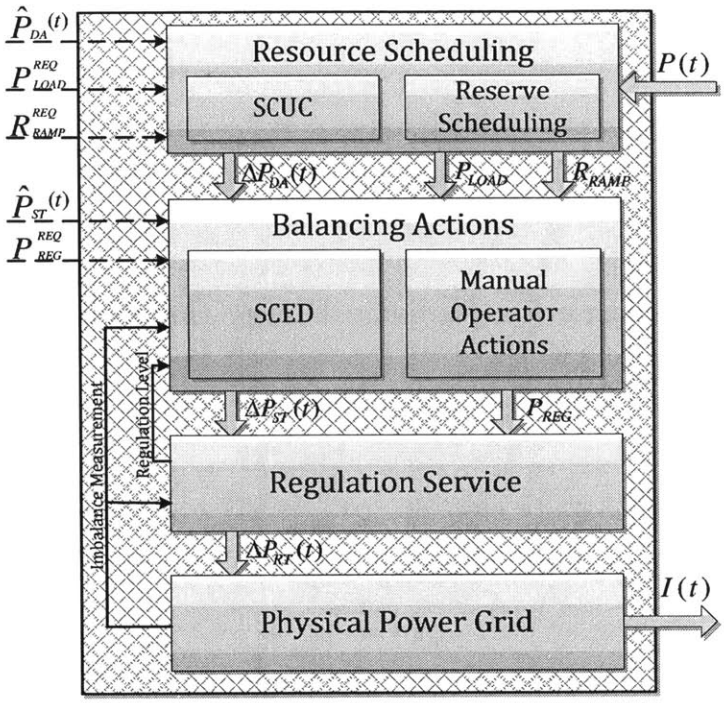

Figure 2-2: Design of Enterprise Control Simulator [1]

2.2 The Need for Unified Demand Side Management Study Approach

The intermittent nature of renewable energy has been discussed in the context of the operational challenges that it brings to electrical grid reliability [6, 113, 114]. The fast fluctuations in renewable energy generation require high ramping capability which must be met by dispatchable energy resources. Additionally, a sudden loss of renewable generation can threaten grid reliability in the absence of adequate generation reserves.

In contrast, DSM with its ability to allow customers to adjust electricity consumption in response to market signals has often been recognized as an efficient way to shave load peaks [115, 116, 117, 118] and mitigate the variable effects of renewable energy [17, 18, 19]. It increases the bulk electric system flexibility [119, 120] and reliability [120, 121, 122, 118] by providing additional dispatchable resources which can potentially offset imbalances caused by renewable energy [22, 23]. DSM has also been

advocated for its ability to increase system efficiency and reduce system costs [20, 21]. By encouraging customers to adjust their electricity consumption in response to market signals, DSM reduces the need for more expensive generators with high ramping capability. Meanwhile, DSM increases the utilization of generating capacities that would have been otherwise idle during off-peak hours, thus reducing the real cost of renewable integration [24]. The electricity supply side, load-reducing customers and non-load-reducing customers all benefit economically from load reductions [25, 26].

The deregulation of electricity markets [123, 37, 35, 124, 125], along with the advances in information and communication technologies [126, 127, 119, 128], has motivated more active DSM programs. As a result, Independent System Operators (ISOs) and Reliability Transmission Organizations (RTOs) have been implementing DSM for its potential to lower market prices, reduce price volatility, improve customer options, and increase the elasticity from wholesale to retail market [45]. Researches on DSM have addressed the minimization of energy consumption, maximization of customer utility, the minimization of customer discomfort, the stabilization of electricity prices, and multi-objective optimizations from the customer side [31, 129, 33, 130, 131, 132, 133]. In addition, there have also been studies on the integration of DSM and renewable uncertainty [134], centralized or distributed demand control algorithms [135, 136, 137, 138, 127, 121, 139], demand-side storage [140, 141], models of customer behavior [142], and prediction of DSM participation potential [143, 144, 145].

However, despite the attention given to DSM, the industrial and academic literature have taken divergent approaches to DSM implementation. A common approach among academic researchers is to maximize social welfare defined as the net benefits from electricity consumption and generation based on the utility of dispatchable demand [30, 31, 32, 33]. In the meantime, the industrial trend has been to introduce "virtual generators" in which customers are compensated for load reductions from baseline electricity consumption [34, 35, 36, 37, 38, 39, 40]. Such a baseline is defined as the counterfactual electricity consumption that would have occurred without DSM and is estimated from historical data from the prior year [41, 42, 43]. The differentce

in contributions of these two methods to system performance remain unclear, especially in the context of the newly proposed enterprise control assessment, and is the topic of the following two chapters.

2.3 Conclusion

This chapter has argued the need for holistic enterprise control assessment methods incorporated with DSM. The requirements for decarbonization, enhanced reliability and transportation electrification motivates new control and automation technologies and consumer participation. Extensive literature has been developed to determine the feasibility of integrating a certain amount of renewable energy. While piece-meal assessment cannot capture all technical challenges, uncoordinated assessments result in costly overbuilt solutions. Most current integration studies are found to have one or more of the following limitations: they are case specific [14], only address a single control function of power grid balancing operations and restricted to the timescale of the chosen function [15], or limited to statistical calculations, which are yet to be validated by simulations [16]. To address the literature gap, a framework for holistic assessment is then proposed in Reference [1] for more robust simulation-based approaches and to enable DSM.

The two different approaches of DSM in academic and industrial literature are summarized and contrasted. The following chapters then quantitatively compare the two DSM implementation methods in a day-ahead wholesale market and in the context of enterprise control.

Chapter 3

Demand Side Management in A Day-Ahead Wholesale Market: A Comparison of Industrial & Social Welfare Approaches

The intermittent nature of renewable energy has been discussed in the context of the operational challenges that it brings to electrical grid reliability. Demand Side Management (DSM) with its ability to allow customers to adjust electricity consumption in response to market signals has often been recognized as an efficient way to mitigate the variable effects of renewable energy as well as to increase system efficiency and reduce system costs. However, the academic & industrial literature have taken divergent approaches to DSM implementation. While the popular approach among academia adopts a social welfare maximization formulation, the industrial practice compensates customers according to their load reduction from a predefined electricity consumption baseline that would have occurred without DSM. This chapter rigorously compares these two different approaches in a day-ahead wholesale market context analytically and in a test case using the same system configuration and mathematical formalism. The comparison of the two models showed that a proper reconciliation of

the two models might make them mitigate the stochastic netload in fundamentally the same way, but only under very specific conditions which are rarely met in practice. While the social welfare model uses a stochastic net load composed of two terms, the industrial DSM model uses a stochastic net load composed of three terms including the additional baseline term. DSM participants are likely to manipulate the baseline in order to receive greater financial compensation. An artificially inflated baseline is shown in this chapter to result in a different resources dispatch, high system costs, and unachievable social welfare, and likely requires more control activity in subsequent layers of enterprise control.

3.1 Motivation & Study Scope

3.1.1 Motivation

Despite recognized importance of Demand Side Management[27, 28, 29], the industrial and academic literature seem to have taken divergent approaches to DSM implementation. A common approach among academic researchers is to maximize social welfare defined as the net benefits from electricity consumption and generation based on the utility of dispatchable demand [30, 31, 32, 33]. In the meantime, the industrial trend has been to introduce "virtual generators" in which customers are compensated for load reductions from baseline electricity consumption [34, 35, 36, 37, 38, 39, 40]. Such a baseline is defined as the counterfactual electricity consumption that would have occurred without DSM and is estimated from historical data from the prior year [41, 42, 43]. The industrial baselines easily involve errors and are most likely to be different from the load forecast. Firstly, the methods of determining the load forecast and industrial baseline are fundamentally different. While the latter is calculated a day in advance based upon sophisticated methods [44], the formulae for baseline are much more basic and determined months in advance [45, 46, 47, 48, 49]. Indeed, it is conceivable that a baseline is set and then the demand side participant makes (static) long-term energy efficiency improvements and then is compensated for

the now guaranteed "load-reduction". As several authors note, the baseline itself is subject to manipulation because DSM participants have greater awareness of their facilities than the regulatory agencies charged with estimating the baseline [50, 51].

3.1.2 Scope

Electricity markets are classified as wholesale or retail markets. Wholesale markets manage generation to transmission, while retail market starts from step-down transformers and distributes electricity to customers on a flat-rate. [52] The procurement and dispatch decision from TJE wholesale market is the result of different parties bidding on various time-scales [53] including in the long-term capacity market, the short-term energy market, and the operating reserve market. Energy markets of day-ahead energy markets and real-time energy markets.

The DSM literature is presented as two classes of energy market problems. The first class of problem is the power scheduling in a day-ahead market, without any guarantee that the dispatchable demands will actually consume the allocated power [113, 115, 19, 128], and the second class is the load shifting in real-time market, where the customers are always able to change their consumption patterns [29, 114, 121, 127, 19, 128]. This chapter belongs to the first category and focuses on comparing the academic and industrial DSM methods in a day-ahead energy market; presented as a unit commitment problem. The underlying assumption is that despite the errors inherent to renewable energy forecast, the forecast model is reliable for the purpose of day-ahead scheduling, and the errors of renewable energy forecast will be corrected in subsequent layers of control in real-time markets and regulation [146, 147]. The day-ahead energy market mechanism as compared to real-time energy markets is described in detail in Section 3.2.1.

3.1.3 Contribution

While the differences between the academic and industrial methods and the errors associated with the baseline have often been a part of policy discussions [50], they have

not been rigorously studied. There have been attempts to incorporate the concept of social welfare into the market auction mechanism, but they are based on conventional dispatch giving no consideration to responsive demands or renewables, and thus renders a very different and much simpler case [148]. For a day-ahead scheduling scenario, a unit commitment problem incorporating DSM has been studied simply from the suppliers side to minimize generation costs [149] or to maximize electric power utility profit [150, 151], and from a markets perspective using either the social welfare [152] and industrial method [153, 154, 155]. This chapter aims to rigorously compare the social welfare and the industrial load reduction approaches and study the effects of an erroneous industrial baseline in a day-ahead wholesale market context using the same system configuration and mathematical formalism.

3.1.4 Chapter Outline

The remainder of this chapter develops in six sections. Section 3.2 summaries highlights from both the academic literature and industrial documents. Section 3.3 presents the mathematical models for both the social welfare and industrial methods of unit commitment with dispatchable demands as well as the model reconciliation. In Section 3.4, the two optimization programs are compared analytically, and the conditions under which the two optimization programs are equivalent are discussed. The test case and methodology are presented in Section 3.5. Section 3.6 presents and discusses the results from the case study for both models with an accurate and erroneous baseline. The chapter concludes in Section 3.7.

3.2 Background

This section first introduces readers to economic dispatch and unit commitment problems. It then summarizes the two contrasting approaches to demand dispatching: social welfare methods often found in academia and load reduction from baseline methods implemented in industry.

3.2.1 Economic Dispatch & Unit Commitment in Wholesale Power Markets

The real-time ISO wholesale market adopts an economic dispatch (ED) problem on the timescale of minutes. Different generating units include nuclear, thermal, hydro, and gas units, and have very different physical limitations and costs characteristics. A traditional ED utilizes all online generating units to meet the total forecast power requirements including customer demands and transmission losses, and allocates the generating power among units such that the total power production costs are minimized [156]. Therefore, a traditional ED problem consists of minimizing generating cost under the constraint of system power balance and physical limitations of generating units, namely capacity and ramping limits [156]. Here, the costs only include that of running the units at the dispatched levels.

The day-ahead ISO wholesale market adopts a unit commitment problem using time periods of an hour or a few hours. In contrast to an ED problem, the goal of which is to determine the optimal generating level, the primary purpose of UC is to choose the appropriate set of online generating units during each time period for the next-day ED. Instead of assuming all available units online, it needs to determine the online or offline state of units. Limitations exist on the frequency each generating unit can be started up or shut down, and costs are associated with starting up or shutting down units. Therefore, two modifications from ED formalism, at a minimum, are needed to form a UC problem: 1) the on/off state of each unit needs to be consistent with the starting and shutting process of the units. 2) the total costs need to include start-up and shut-down costs in addition to operating costs. [156]

Another difference worth special attention is that while transmission losses explicitly exist in ED, it does so less frequently in UC. The reason is that UC usually dispatches over long time periods and is only based on coarse forecasts and does not provide accurate generating levels. Therefore, the transmission loss is not expected to affect the UC greatly but greatly complicates the optimization, and is usually omitted in UC problems [156, 157, 158, 146, 159, 160, 161].

3.2.2 Academic Literature

A popular approach in the academic literature is to adopt a maximal social welfare problem formulation. Elastic demand is characterized by its utility U – the benefit from electricity consumption, and generation is characterized by its cost C [156]. The maximum social welfare determines the dispatch schedule and price for suppliers and customers at the same time[31, 150]. In an economic dispatch context, social welfare has been defined in textbooks as[156]:

$$SW(P_G, P_D) = \sum_{j=1}^{m} U_j(P_{Dj}) - \sum_{i=1}^{n} C_i(P_{Gi}) \tag{3.1}$$

where P_D and P_G represent the individual demands and generators respectively; m and n represent the number of demands and generators. Assuming lossless transmission, the system power balance constraint becomes [156]:

$$\sum_{i=1}^{n} P_{Gi} = \sum_{j=1}^{m} P_{Dj} \tag{3.2}$$

The objective function in (3.1) and the constraint in (3.2) constitute the simplest form of social welfare maximization. As mentioned and cited in the introduction, the electricity industry implements a different approach.

3.2.3 Industrial Practice

The industrial approach to dispatching demand minimizes the total cost of dispatchable generation and virtual generation. A curtailment service provider (CSP) represents the demand units participating in the wholesale energy market. Each CSP has an "administratively-set" electricity consumption baseline as an estimate of consumption without DSM incentives and from which load reductions are measured. The CSP can participate in one of several wholesale energy markets [162]; one of them being the Day-Ahead Scheduling Reserve Market (DASR) where generation suppliers, load serving entities, and CSPs bid through an ISO/RTO [53]. The bidding process

determines the dispatched resources as well as the electricity price for the next day [39]. Accepted load reductions are obliged to commit and are subsidized by ISO/RTO based on the bidding price compared to the Locational Marginal Pricing (LMP) and the Retail Rates (GT) [26]. While very much discouraged, customers have an implicit incentive to surreptitiously inflate the administrative baseline for greater compensation. For example, the customers can artificially increase their electricity consumption when baselines are being evaluated [50]. Customers who anticipate to reduce loads regardless of DSM are also more likely to be attracted to participate [50]. Another example is customers having multiple facilities shift loads between facilities to create false load reductions [50]. Successful baseline manipulation may cause generation relocation and inefficient price information [50].

3.3 Mathematical Models

This section now describes the mathematical formulation for both the social welfare and industrial load reduction models.

3.3.1 Social Welfare Maximization

The formulation of maximal social welfare problem is as follows. Unlike the economic dispatch problem presented in Section 3.2.2, the unit commitment model schedules the dispatchable resources and determines their states over multiple time intervals. The optimization program in Section 3.2.2 also assumed that all generators and loads are dispatchable. For greater practicality, this assumption is relaxed so that stochastic generation (i.e. renewable energy) and stochastic demand (i.e. conventional load) can be included. These are taken as fixed exogenous quantities whose costs and utilities are independent from dispatch decisions and which must be balanced by dispatchable generation and demand units. The objective function to maximize is the total social welfare $\mathcal{W}$ is given by [163]:

$$\mathcal{W} = \sum_{T=1}^{N_T} \left[\sum_{j=1}^{N_{DC}} \mathcal{U}_{DCj}(P_{DCjT}) - \sum_{i=1}^{N_{GC}} \mathcal{C}_{GCi}(P_{GCiT}) \right] \tag{3.3}$$

where both the demand utility $\mathcal{U}_{DCj}$ and generation cost $\mathcal{C}_{GCi}$ have a startup, a shutdown, and a running component shown in Equation (3.4) and Equation (3.5) [163].

$\forall i = 1, ..., N_{GC}, \forall j = 1, ..., N_{DC}, \forall T = 1, ..., N_T :$

$$\mathcal{C}_{GCi}(P_{GCiT}) = u_{GCiT}(\mathcal{S}_{GCi}) + v_{GCiT}(\mathcal{D}_{GCi}) + w_{GCiT}\left[\mathcal{R}_{GCi}(P_{GCiT})\right] \tag{3.4}$$

$$\mathcal{U}_{DCj}(P_{DCjT}) = u_{DCjT}(\mathcal{S}_{DCj}) + v_{DCjT}(\mathcal{D}_{DCj}) + w_{DCjT}\left[\mathcal{R}_{DCj}(P_{DCjT})\right] \tag{3.5}$$

where the running cost for generators $\mathcal{R}_{GCit}$ and running utility for demands $\mathcal{R}_{DCjt}$ are modeled as quadratic functions to capture the change in marginal costs and marginal utilities [163].

$\forall i = 1, ..., N_{GC}, \forall j = 1, ..., N_{DC}, \forall T = 1, ..., N_T :$

$$\mathcal{R}_{GCi}(P_{GCiT}) = A_{GCi}(P_{GCiT})^2 + B_{GCi}(P_{GCiT}) + \zeta_{GCi} \tag{3.6}$$

$$\mathcal{R}_{DCj}(P_{DCjT}) = A_{DCj}(P_{DCjT})^2 + B_{DCj}(P_{DCjT}) + \zeta_{DCj} \tag{3.7}$$

Acquiring a reliable utility model in day-ahead wholesale market necessitates accurate forecast of utility functions and is not always easy to achieve in that it depends on customers providing information for the next day. Not only are errors inherent to utility forecast, but the heterogeneity of customers also brings difficulty to curtailment service providers serving aggregated groups of customers.[31] However, it is still considered a good method and used commonly among academic studies for two reasons. Firstly, customers do not have incentives to report false utility information. Remember utility is defined as the benefits a customer gets from consuming electricity, and over-stating utility results in the customer over-buying and wasting money on excess electricity. On the other hand, under-stating utility leads to not procuring enough electricity. Secondly the customers are expected to be well aware of their utility information and one day is a considered a short period in advance and helps

to mitigate forecast errors.

The objective function is optimized subject to the system power balance constraint in Equation (3.8), and the physical capacity constraint for both the dispatchable generators in Equation (3.9) and dispatchable demands in Equation (3.10). The ramping rate is defined as the change in generation power from the last time interval as in Equation (3.11a). In a simplified model, the ramping of generators is assumed to be linear. This approximation has been commonly adopted among large-scale electrical grid studies and is described in textbooks[156]. The physical downward and upward generation ramping limits are implemented with the lower and upper constraints as in Equation (3.11b). Similarly, the ramping constraints of dispatchable demands are found in Equation (3.12). The logical constraints of dispatchable generators and dispatchable demands are shown in Equations (3.13) and (3.14) respectively [163].
$\forall i = 1, ..., N_{GC}, \forall j = 1, ..., N_{DC}, \forall T = 1, ..., N_T$:

$$\sum_{i=1}^{N_{GC}} P_{GCiT} - \sum_{j=1}^{N_{DC}} P_{DCjT} = \sum_{k=1}^{N_{DS}} \hat{P}_{DSkT} - \sum_{l=1}^{N_{GS}} \hat{P}_{GSlT} \tag{3.8}$$

The power balance constraint is composed of terms: the power injection for the dispatchable and stochastic generating and demand units. As is commonly found in the literature, the power system losses are neglected in UC formalism but compensated by the load following reserves term [156, 157, 158, 146, 159, 160, 161]. The reader is referred to [164] for one approach to the incorporation of losses. The load following and ramping reserves are calculated for subsequent ED control according to the methods provided in references [146, 147]. In this work, the load following reserve is set to 20% of peakload, a very conservative amount to ensure load tracking in real-time market and imposes no active constraints in the unit commitment problem.

$$w_{GCiT} * \underline{P_{GCi}} \leq P_{GCiT} \leq w_{GCiT} * \overline{P_{GCi}} \tag{3.9}$$

$$w_{DCjT} * \underline{P_{DCj}} \leq P_{DCjT} \leq w_{DCjT} * \overline{P_{DCj}} \tag{3.10}$$

The maximum capacity of each dispatchable demand unit is determined one-day ahead using the sophisticated method of load forecasting, contrasted to the industrial baseline which is usually contracted months or even years ahead.

$$R_{GCiT} = P_{GCiT} - P_{GCi(T-1)} \tag{3.11a}$$

$$\underline{R_{GCi}} \leq R_{GCiT} \leq \overline{R_{GCi}} \tag{3.11b}$$

$$R_{DCjT} = P_{DCjT} - P_{DCj(T-1)} \tag{3.12a}$$

$$\underline{R_{DCj}} \leq R_{DCjT} \leq \overline{R_{DCj}} \tag{3.12b}$$

$$w_{GCiT} = w_{GCi(T-1)} + u_{GCiT} - v_{GCiT} \tag{3.13}$$

$$w_{DCjT} = w_{DCj(T-1)} + u_{DCjT} - v_{DCjT} \tag{3.14}$$

3.3.2 Industrial Practice: Cost Minimization with Demand Baseline

The formulation of the industrial Unit Commitment model is as follows. Much like the social welfare model, the industrial unit commitment model determines the set-points for all dispatchable resources. In contrast, however, the optimization goal industrial approach is to minimize the total cost of dispatchable generators and virtual generators over all time intervals of the SCUC period, where the cost of virtual generation is the compensation paid to the customers for reducing their consumption from predefined demand baseline. The industrial demand side mangement objective

is given in Equation (3.15) [163].

$$\sum_{T=1}^{N_T}\left[\sum_{i=1}^{N_{GC}}\mathcal{C}_{GCi}(P_{GCiT})+\sum_{j=1}^{N_{DC}}\mathcal{C}_{DCj}(\tilde{P}_{DCjT}-P_{DCjT})\right] \tag{3.15}$$

where the costs of the dispatchable generation remain the same as in Equation (3.4) and the costs of dispatchable demand shown in Equation (3.16) [163] also have startup, shutdown, and running cost.

$\forall i=1,...,N_{GC},\forall j=1,...,N_{DC},\forall T=1,...,N_T:$

$$\begin{aligned}&\mathcal{C}_{DCj}(\tilde{P}_{DCjT}-P_{DCjT})=\\&\mu_{DCjT}(\mathbb{S}_{DCj})+\nu_{DCjT}(\mathbb{D}_{DCj})+\omega_{DCjT}\left[\mathbb{R}_{DCj}(\tilde{P}_{DCjT}-P_{DCjT})\right]\end{aligned} \tag{3.16}$$

The running cost is similarly modeled as a quadratic function of the load reduction from the baseline.

$\forall i=1,...,N_{GC},\forall j=1,...,N_{DC},\forall T=1,...,N_T:$

$$\begin{aligned}&\mathbb{R}_{DCj}(\tilde{P}_{DCjT}-P_{DCjT})=\\&\mathbb{A}_{DCj}(\tilde{P}_{DCjT}-P_{DCjT})^2+\mathbb{B}_{DCj}(\tilde{P}_{DCjT}-P_{DCjT})+\xi_{DCj}\end{aligned} \tag{3.17}$$

The objective function is optimized subject to same system power balance constraint in Equation (3.8)[163]. Both the dispatchable generation and virtual generation are subject to the capacity limits in Equations (3.9) and (3.18a) respectively, the ramping limits in Equations (3.11) and (3.12) respectively, and the logical constraints in Equations (3.13) and (3.19) respectively [163].

$\forall j=1,...,N_{DC},\forall T=1,...,N_T$

$$\omega_{DCjT}*\underline{\tilde{P}_{DCjT}-P_{DCjT}}\leq\tilde{P}_{DCjT}-P_{DCjT} \tag{3.18a}$$

$$\tilde{P}_{DCjT}-P_{DCjT}\leq\omega_{DCjT}*\overline{\tilde{P}_{DCjT}-P_{DCjT}} \tag{3.18b}$$

$$\overline{w}_{DCjT} = \overline{u}_{DCj(T-1)} + \overline{u}_{DCjT} - \overline{v}_{DCjT} \tag{3.19}$$

The industrial method dictates that the load reduction does not exceed the baseline. A full reduction corresponds to the magnitude of the baseline. As mentioned in Section 3.1 & 3.3.1, the baselines are determined months or even years ahead based on electricity consumption history data and are subject to manipulation, and therefore are more prone to errors than its counterpart of maximum dispatchable demand forecast in social welfare model.

3.3.3 Model Reconciliation

For fair comparison of the two models, the constraints and utility/cost functions of dispatchable demands in the two models need to be reconciled. The virtual generation cost function in the industrial model is reconciled with the utility function of the corresponding dispatchable demand unit such that the loss in utility in the SW model is equal to the change in virtual generation cost. The economics rationale for this is that the customers are only willing to cut down electricity consumption if their marginal loss in utility is subsidized by the marginal cost in virtual generation[163].
$\forall j = 1, ..., N_{DC}$:

$$\begin{aligned} &-\mathcal{U}_{DCj}(P_{DCj}) + \mathcal{U}_{DCi}(P_{DCj} + \delta P_{DCj}) = \\ &\mathcal{C}_{DCj}(\tilde{P}_{DCj} - P_{DCj}) - \mathcal{C}_{DCj}(\tilde{P}_{DCj} - P_{DCj} - \delta P_{DCj}) \end{aligned} \tag{3.20}$$

Rearranging quadratic and linear terms in Equation (3.20) yields Equation (4.13)[163]. It shows that the cost function of load reduction is dependent on the choice of baseline.
$\forall j = 1, ..., N_{DC}$:

$$\begin{aligned} \mathbb{A}_j &= -A_j \\ \mathbb{B}_j &= 2 * A_j * \tilde{P}_{DCj} + B_j \end{aligned} \tag{3.21}$$

The maximum load reduction is assumed to occur when dispatchable demand is operating at its minimum level. Now that the two optimization programs are well defined and reconciled with each other, the next section proceeds to comparing them with each other.

3.4 Analytical Comparison of the Two Optimization Models

In this section, the social welfare maximization method and load reduction optimization method are compared analytically using the function reconciliation developed in Subsection 3.3.3. As a conclusion, the two models are shown to yield different optima in all but a few cases. The equivalence conditions require that the industrial baseline is equal to the maximum capacity and that the dispatchable demand startup and shutdown costs are ignored. However, these conditions are seldom true, and therefore the two models will very likely generate different results in practice. The analytical comparison is conducted in two steps first as an economic dispatch problem in Subsection 3.4.1 then as a unit commitment problem in Subsection 3.4.2.

3.4.1 Analytical Comparison in Economic Dispatch

This subsection compares the two models in an economic dispatch scenario where only one time interval is analyzed. Ramping limits and binary variable logical constraints span multiple time intervals. They are neglected here but reintroduced in subsequent sections. The Lagrangian functions for social welfare and industrial programs are presented in Subsubsection 3.4.1 and 3.4.1 respectively. They are compared in Subsubsection 3.4.1 and found to be equivalent if and only if the industrial baseline is equal to the maximum capacity in social welfare model.

Social Welfare Model Lagrangian Function

In an economic dispatch problem, the social welfare model reduces to the maximization of total social welfare over all time intervals in Equation (3.3) to the maximization on one time interval:

$$\sum_{j=1}^{N_{DC}} \mathcal{U}_{DCj}(P_{DCjt}) - \sum_{i=1}^{N_{GC}} \mathcal{C}_{GCi}(P_{GCit}) \tag{3.22}$$

subject to the power balance equality constraint for all generators and dispatchable demands;

$$\sum_{i=1}^{N_{GC}} P_{GCit} - \sum_{j=1}^{N_{DC}} P_{DCjt} = \sum_{k=1}^{N_{DS}} \hat{P}_{DSkt} - \sum_{l=1}^{N_{GS}} \hat{P}_{GSlt} \tag{3.23}$$

and the capacity inequality constraints
$\forall i = 1, ..., N_{GC}, \forall j = 1, ..., N_{DC}$:

$$\underline{P_{DCj}} \leq P_{DCjt} \leq \overline{P_{DCj}} \tag{3.24a}$$

$$\underline{P_{GCi}} \leq P_{GCit} \leq \overline{P_{GCi}} \tag{3.24b}$$

The Lagrangian function of the social welfare model can then be written as

$$\begin{aligned}
L(P_{DCjt}, P_{GCit}, \lambda) &= \sum_{i=1}^{N_{GC}} A_{GCi}(P_{GCit})^2 + \sum_{i=1}^{N_{GC}} B_{GCi}(P_{GCit}) + \sum_{i=1}^{N_{GC}} \zeta_{GCi} \\
&- \sum_{j=1}^{N_{DC}} A_{DCj}(P_{DCjt})^2 - \sum_{j=1}^{N_{DC}} B_{DCj}(P_{DCjt}) - \sum_{j=1}^{N_{DC}} \zeta_{DCj} \\
&- \lambda\Big[\Big(\sum_{i=1}^{N_{GC}} P_{GCit} - \sum_{j=1}^{N_{DC}} P_{DCjt}\Big) - \Big(\sum_{k=1}^{N_{DS}} \hat{P}_{DSkt} - \sum_{l=1}^{N_{GS}} \hat{P}_{GSlt}\Big)\Big] \\
&- \mu_1(P_{GCit} - \overline{P_{GCi}}) - \mu_2(P_{GCit} - \underline{P_{GCi}}) \\
&- \mu_3(P_{DCjt} - \overline{P_{DCj}}) - \mu_4(P_{DCjt} - \underline{P_{DCj}})
\end{aligned} \tag{3.25}$$

The optimal solution can be solved from the system of equations in (3.26) by equating the partial derivative of each variable to zero (Equation (3.26a) - (3.26c)) and including the complementary equations for all inequality constraints (Equation (3.26d) - (3.26g)):

$\forall i = 1, ..., N_{GC}, \forall j = 1, ..., N_{DC}, \forall t = 1, ..., N_t$:

$$\frac{\partial L}{\partial P_{GCit}} = 2A_{GCi}P_{GCit} + B_{GCi} - \lambda - \mu_1 - \mu_2 = 0 \tag{3.26a}$$

$$\frac{\partial L}{\partial P_{DCjt}} = -2A_{DCj}P_{DCjt} - B_{DCj} + \lambda - \mu_3 - \mu_4 = 0 \tag{3.26b}$$

$$\Big(\sum_{i=1}^{N_{GC}} P_{GCit} - \sum_{j=1}^{N_{DC}} P_{DCjt}\Big) - \Big(\sum_{k=1}^{N_{DS}} \hat{P}_{DSkt} - \sum_{l=1}^{N_{GS}} \hat{P}_{GSlt}\Big) = 0 \tag{3.26c}$$

$$\mu_1(P_{GCit} - \overline{P_{GCi}}) = 0, \qquad \mu_1 \leq 0 \tag{3.26d}$$

$$\mu_2(P_{GCit} - \underline{P_{GCi}}) = 0, \qquad \mu_2 \geq 0 \tag{3.26e}$$

$$\mu_3(P_{DCjt} - \overline{P_{DCj}}) = 0, \qquad \mu_3 \leq 0 \tag{3.26f}$$

$$\mu_4(P_{DCjt} - \underline{P_{DCj}}) = 0, \qquad \mu_4 \geq 0 \tag{3.26g}$$

Industrial Model Lagrangian Function

Similarly, the industrial model reduces the minimization of total costs over all time intervals in Equation (3.15) to the minimization of costs on one interval:

$$\sum_{i=1}^{N_{GC}} \mathcal{C}_{GCi}(P_{GCit}) + \sum_{j=1}^{N_{DC}} \mathcal{C}_{DCj}(\tilde{P}_{DCj} - P_{DCjt}) \tag{3.27}$$

subject to the same power balance constraint as in Equation (3.23) and capacity limits

$\forall i = 1, ..., N_{GC}, \forall j = 1, ..., N_{DC}, \forall t = 1, ..., N_t :$

$$\underline{P_{GCi}} \leq P_{GCit} \leq \overline{P_{GCi}} \tag{3.28a}$$

$$\underline{\tilde{P}_{DCj} - P_{DCj}} \leq \tilde{P}_{DCj} - P_{DCjt} \leq \overline{\tilde{P}_{DCj} - P_{DCj}} \tag{3.28b}$$

The Lagrangian function for the industrial optimization is then written as

$$\begin{aligned}
L_(P_{DCjt}, P_{GCit}) &= \sum_{i=1}^{N_{GC}} A_{GCi}(P_{GCit})^2 + \sum_{i=1}^{N_{GC}} B_{GCi}(P_{GCit}) + \sum_{i=1}^{N_{GC}} \zeta_{GCi} \\
&+ \sum_{j=1}^{N_{DC}} \mathbb{A}_{DCj}(\tilde{P}_{DCjt} - P_{DCjt})^2 + \sum_{j=1}^{N_{DC}} \mathbb{B}_{DCj}(\tilde{P}_{DCjt} - P_{DCjt}) + \sum_{j=1}^{N_{DC}} \xi_{DCj} \\
&- \lambda\Big[\Big(\sum_{i=1}^{N_{GC}} P_{GCit} - \sum_{j=1}^{N_{DC}} P_{DCjt}\Big) - \Big(\sum_{k=1}^{N_{DS}} \hat{P}_{DSkt} - \sum_{l=1}^{N_{GS}} \hat{P}_{GSlt}\Big)\Big] \\
&- \mu_1(P_{GCit} - \overline{P_{GCi}}) - \mu_2(P_{GCit} - \underline{P_{GCi}}) \\
&- \mu_3\Big[(\tilde{P}_{DCj} - P_{DCjt}) - \overline{\tilde{P}_{DCj} - P_{DCj}}\Big] \\
&- \mu_4\Big[(\tilde{P}_{DCj} - P_{DCjt}) - \underline{\tilde{P}_{DCj} - P_{DCj}}\Big]
\end{aligned} \tag{3.29}$$

The optimal solution can be obtained by equating the partial derivative of Lagrangian function with respect to each variable to zero and solving the complementary conditions simultaneously. Substituting the reconciled virtual generation cost function coefficients Equation (4.13) into the partial derivative of the Lagrangian function with respect to the dispatchable generation levels yields Equations 3.30:

$$\frac{\partial L_2}{\partial P_{DCjt}} = 2\mathbb{A}_{DCj}(\tilde{P}_{DCj} - P_{DCjt}) + \mathbb{B}_{DCj} + \lambda - \mu_{1j} + \mu_{2j} = 0 \tag{3.30}$$

The resulting system of equations required to find the industrial optimal solution is:
$\forall i = 1, ..., N_{GC}, \forall j = 1, ..., N_{DC}, \forall t = 1, ..., n_t$:

$$\frac{\partial L}{\partial P_{GCit}} = 2A_{GCi}P_{GCit} + B_{GCi} - \lambda - \mu_1 - \mu_2 = 0 \tag{3.31a}$$

$$\frac{\partial L}{\partial P_{DCjt}} = -2A_{DCj}P_{DCjt} - B_{DCj} + \lambda + \mu_3 + \mu_4 = 0 \tag{3.31b}$$

$$\Big(\sum_{i=1}^{N_{GC}} P_{GCit} - \sum_{j=1}^{N_{DC}} P_{DCjt}\Big) - \Big(\sum_{k=1}^{N_{DS}} \hat{P}_{DSkt} - \sum_{l=1}^{N_{GS}} \hat{P}_{GSlt}\Big) = 0 \tag{3.31c}$$

$$\mu_1(P_{GCit} - \overline{P_{GCi}}) = 0, \qquad \mu_1 \leq 0 \tag{3.31d}$$

$$\mu_2(P_{GCit} - \underline{P_{GCi}}) = 0, \qquad \mu_2 \geq 0 \tag{3.31e}$$

$$\mu_3\Big[(\tilde{P}_{DCj} - P_{DCjt}) - \overline{\tilde{P}_{DCj} - P_{DCj}}\Big] = 0, \qquad \mu_3 \leq 0 \tag{3.31f}$$

$$\mu_4\Big[(\tilde{P}_{DCj} - P_{DCjt}) - \underline{\tilde{P}_{DCj} - P_{DCj}}\Big] = 0, \qquad \mu_4 \geq 0 \tag{3.31g}$$

Equivalance Conditions

Equations (3.26) and Equation (3.31) are then compared. A close inspections shows that Equations (3.26a) to (3.26e) are the same as their industrial model counterparts in Equations (3.31a) to (3.31e). Furthermore, Equation (3.26f)&(3.26g) are equivalent to Equation (3.31f)&(3.31g) if the conditions in Equation (3.32) are met.
$\forall i = 1, ..., N_{GC}, \forall j = 1, ..., N_{DC}, \forall t = 1, ..., N_t$:

$$\tilde{P}_{DCj} - \underline{\tilde{P}_{DCj} - P_{DCjt}} = \overline{P_{DCj}} \tag{3.32a}$$

$$\tilde{P}_{DCj} - \overline{\tilde{P}_{DCj} - P_{DCj}} = \underline{P_{DCj}} \tag{3.32b}$$

In other words, the two optimization programs are the same if and only if the industrially defined minimum load reduction $\underline{\tilde{P}_{DCj} - P_{DCjt}}$ occurs at the highest dispatchable demand level in the social welfare model $\overline{P_{DCj}}$, and the highest load reduction $\overline{\tilde{P}_{DCj} - P_{DCj}}$ occurs at the lowest dispatchable demand level in the social welfare model $\underline{P_{DCj}}$.

If it is assumed that the minimum reduction $\underline{\tilde{P}_{DCj} - P_{DCjt}}$ is zero when the customers do not reduce their electricity consumption. Equation (3.32a) simplifies to (3.33a).

$\forall i = 1, ..., N_{GC}, \forall j = 1, ..., N_{DC}$:

$$\tilde{P}_{DCj} = \overline{P_{DCj}} \tag{3.33a}$$

$$\tilde{P}_{DCj} - \overline{\tilde{P}_{DCj} - P_{DCj}} = \underline{P_{DCj}} \tag{3.33b}$$

With the above assumption, if the coefficients are properly reconciled as in Equation (4.13), the two optimization programs are equivalent if the baseline is equal to the maximum capacity in the social welfare model (Equation (3.33a)), and the maximum load reduction occurs when the dispatchable demand is running at its minimum level (Equation (3.33b)).

3.4.2 Analytical Comparison in Unit Commitment

This section now returns to the comparison the models as unit commitment problems.

First, the startup and shutdown costs of dispatchable demands have completely different physical meanings in the two optimization programs and including them in the optimization will result in different dispatch levels from the two models. In the social welfare model, the startup cost and shutdown cost represent the costs to turn the corresponding load facility on and off respectively. However, in the industrial

model, the startup cost occurs when load reduction starts from the baseline, and the shutdown cost occurs when the load returns to the baseline from a lower consumption level. Therefore, only when the startup and shutdown costs are ignored can the equivalence conditions in Equation (3.33) be extended to unit commitment.

With this insight in mind, ramping and logical constraints can be addressed for the two models. The solutions in the social welfare model are always feasible in the industrial model if Equation (3.33) is met, and vice versa. Intuitively, the two models should have the same results because the social welfare loss from the optimal point in social welfare model equals the additional cost in the industrial model. Let P^*_{GCiT} and P^*_{DCjT} denote the optimal solution in the social welfare problem and P_{GCiT} and P_{DCjT} be any other dispatch level. Symbolically,

$$\mathcal{W}(P^*_{GCiT}, P^*_{DCjT}) - \mathcal{W}(P_{GCiT}, P_{DCjT}) \geq 0 \tag{3.34}$$

If the optimal point also yields the minimum total system costs then two model are equivalent under the previously described conditions.

Substituting the social welfare definition in Equation (3.3) and the dispatchable demand utility functions in Equation (3.5)&(3.7) into Equation (3.34) and eliminating all dispatchable demand startup and shutdown costs gives

$$\begin{aligned}&\sum_{T=1}^{N_T}\sum_{j=1}^{N_{DC}}\left[A_{DCj}({P^*_{DCjT}}^2 - {P_{DCjT}}^2) + B_{DCj}(P^*_{DCjT} - P_{DCjT})\right]\\&-\sum_{T=1}^{N_T}\sum_{i=1}^{N_{GC}}\left[\mathcal{C}_{GCi}(P^*_{GCiT}) - \mathcal{C}_{GCi}(P_{GCiT})\right] \geq 0\end{aligned} \tag{3.35}$$

Turning to the industrial load reduction method, the difference in total system costs between the social optimal point and any other point is

$$\begin{aligned}&\sum_{T=1}^{N_T}\left[\sum_{i=1}^{N_{GC}}\mathcal{C}_{GCi}(P^*_{GCiT}) + \sum_{j=1}^{N_{DC}}\mathcal{C}_{DCj}(\tilde{P}_{DCj} - P^*_{DCjT})\right]\\&-\sum_{T=1}^{N_T}\left[\sum_{i=1}^{N_{GC}}\mathcal{C}_{GCi}(P_{GCiT}) + \sum_{j=1}^{N_{DC}}\mathcal{C}_{DCj}(\tilde{P}_{DCj} - P_{DCjT})\right]\end{aligned} \tag{3.36}$$

Similarly, substituting in the cost of virtual generation in Equation (3.16 & 3.17) and eliminating virtual generation startup and shutdown cost gives

$$\begin{aligned}
&\sum_{T=1}^{N_T}\sum_{i=1}^{N_{GC}}\Big[\mathcal{C}_{GCi}(P^*_{GCiT}) - \mathcal{C}_{GCi}(P_{GCiT})\Big] \\
&+\sum_{T=1}^{N_T}\sum_{j=1}^{N_{DC}}\Big[\mathbb{A}\Big((\tilde{P}_{DCj} - P^*_{DCjT})^2 - (\tilde{P}_{DCj} - P_{DCjT})^2\Big) \\
&+\mathbb{B}\Big((\tilde{P}_{DCj} - P^*_{DCjT}) - (\tilde{P}_{DCj} - P_{DCjT})\Big)\Big]
\end{aligned} \tag{3.37}$$

Substituting in the reconciled coefficients in Equation (4.13) results in the negative of the social welfare optimal solution condition in Equation (3.35), so

$$\begin{aligned}
&\sum_{T=1}^{N_T}\Big[\sum_{i=1}^{N_{GC}}\mathcal{C}_{GCi}(P^*_{GCiT}) + \sum_{j=1}^{N_{DC}}\mathcal{C}_{DCj}(\tilde{P}_{DCj} - P^*_{DCjT})\Big] \\
&-\sum_{T=1}^{N_T}\Big[\sum_{i=1}^{N_{GC}}\mathcal{C}_{GCi}(P_{GCiT}) + \sum_{j=1}^{N_{DC}}\mathcal{C}_{DCj}(\tilde{P}_{DCjT} - P_{DCjT})\Big] \leq 0
\end{aligned} \tag{3.38}$$

This means that P^*_{DCjT} and P^*_{DCjT} always have less system costs. In other words, the social welfare optimal dispatch level is also the industrial optimal solution.

In summary, the two models are only equivalent under specific conditions; namely the startup and shutdown costs of dispatchable demands have to be neglected, the minimum and maximum load reduction occur when the dispatchable demand unit is running at its maximum and minimum capacity in the social welfare respectively. Not meeting these conditions will result in different dispatch levels from the two models.

3.5 Case Study

The case study consists of a day-ahead unit commitment simulation in a wholesale market for both the social welfare and industrial DSM methods. For fairness of comparison, the same system configuration and data are used to compare the two optimization programs presented in the previous section. The results are studied for their differences in the dispatched energy resources, resulting social welfare, and

system costs. Data is drawn from the *Reliability Test System(RTS)-1996*[2, 3] and the Bonneville Power Administration (BPA) website [165]. The following subsections describe the simulation parameters in detail.

3.5.1 Time Scale

In the study of a day-ahead UC program, the time span is 24 hours. A 1-hour time interval is chosen for the case study [163].

3.5.2 Stochastic Generation, Stochastic Demand

The stochastic generation is taken as the renewable energy generation [163]. Because it only appears in the power system balance constraint, only aggregate renewable energy generation is required. It is drawn from the wind forecast data published on the Bonneville Power Administration (BPA) website for May 12, 2013[165]. To have the load better suit the dispatchable energy resources in the simulation, the data was scaled up to 1.6 times of its values. The raw data for the load forecast has a sampling resolution of 5 minutes, and was down sampled by taking hourly averages. The resulting numbers are provided in Table 3.1.

Similarly, the stochastic demand is taken as the conventional load [163]. Its aggregate value is drawn from the BPA load repository for the same day[165], scaled by the same factor, and downsampled to an hourly resolution. The resulting numbers are provided in Table 3.1 and only apply to the demand side units not participating in the DSM program.

3.5.3 Dispatchable Generation,Dispatchable Demands, & Demand Baseline

Dispatchable generators refer to the generation plants that can be fully controlled. Their dispatch level is a key quantity of interest in this study. Dispatchable demands come from the DSM participants and are assumed to be fully controllable without error.

Table 3.1: Stochastic Demand & Stochastic Generation Levels in Unit Commitment

Hour of the Day	1	2	3	4	5	6	7	8	9	10	11	12
Load Forecast 05/15/2013 (MW)	8347	8036	7795	7691	7711	7827	7994	8487	9186	9515	9626	9648
Wind Forecast 05/15/2013 (MW)	3163	2528	2518	2861	3037	2878	3231	3576	3320	3242	3471	3335
Hour of the Day	13	14	15	16	17	18	19	20	21	22	23	24
Load Forecast 05/15/2013 (MW)	9679	9618	9594	9621	9657	9701	9728	9753	9927	9753	9132	8498
Wind Forecast 05/15/2013 (MW)	3343	3623	4009	4522	4716	5028	4360	4253	3412	2421	2136	2160

[165]

Table 3.2: Dispatchable Generator Parameters[2, 3]

N_{GC}	72									
Unit Type	Generator Index	$\overline{P_{GCi}}$ (MW)	$\underline{P_{GCi}}$ (MW)	$\overline{R_{GCi}}$ (MW/MI)	$\underline{R_{GCi}}$ (MW/MI)	ζ_{GCi} ($)	B_{GCi} ($/MW)	A_{GCi} ($/$MW^2$)	S_{GCi} ($)	D_{GCi} ($)
U12	16,17,18,19,20,49,50,51,52,53,82,83,84,85,86	12	2.4	1	-1	37.8	26.8	10	874	0
U20	01,02,05,06,34,35,38,39,67,68,71,72	20	4.0	3	-3	163.3	39.2	10	115	0
U76	03,04,07,08,36,37,40,41,69,70,73,74	76	15.2	2	-2	151.2	13.5	3	1401	0
U100	09,11,42,44,75,77	100	20.0	7	-7	312.8	21.7	0.1	5750	0
U155	21,22,31,32,54,55,64,65,87,88,97,98	155	31.0	3	-3	210.4	11.0	0.1	611	0
U197	45,46,47,78,79,80	197	39.4	3	-3	315.1	21.9	0.01	10189	0
U350	33,66,99	350	70.0	4	-4	181.0	11.0	0.01	4500	0
U400	23,24,56,57,89,90	400	80.0	20	-20	343.7	5.6	0.01	4700	0

Table 3.3: Dispatchable Demand Unit Parameters

index	$\underline{P_{DCj}}$ (MW)	$\overline{R_{DCj}}$ (MW/MI)	$\underline{R_{DCj}}$ (MW/MI)	ζ($)	B_j ($/MW)	A_j ($/$MW^2$)	S_{DCj} ($)	D_{DCj} ($)
j	0	$\overline{P_{DCj}}/20$	-$\overline{P_{DCj}}/20$	0	112.5	-0.5	0	0

Dispatchable generator parameters are listed in Table 3.2[2]. The startup cost is based on hot start. Slack generators, regulating generators and hydro generators do not participate in unit commitment, and therefore are excluded from the table. The system has a total dispatchable generating capacity of 8424 MW available for day-ahead unit commitment. Ramping is assumed to occur during the first five minutes of every hour.

For the sake of simplicity, a dispatachable demand unit was assumed to exist on each bus [163]. The utility function coefficients for all the dispatchable demand units are assumed to be equal and time-invariant. They are provided in Table 3.3. The minimum and maximum capacity limit of each dispatchable demand unit is assumed to be zero and 9.6% of the peak load published for that bus in the RTS-1996 test case. It is assumed that each dispatchable demands needs 20 minutes to fully ramp between zero and maximum consumption. No load recovery is considered because the customers are assumed to base their electricity consumption only on the current utility and electricity cost. As mentioned in Subsection 3.4.2, the startup and shutdown costs have entirely different physical meanings in the social welfare and industrial DSM models. For fairness of comparison, the startup and shutdown costs are neglected (i.e. set to zero) in this case study.

This work sets the true baseline to a time-invariant value equal to 9.6% of the peak demand [163]. Furthermore, this work assumes this error-free baseline is equal to the maximum capacity of the dispatchable demand unit in the social welfare model. $\tilde{P}_{DCj} = \overline{P}_{DCj}$. The erroneous baseline was set to 120% of its true value to emphasize its impact. This has the implicit effect of allowing demand units to have a maximum load reduction (capacity) of 120% as that found in the social welfare model.

3.5.4 Computational Methods

The optimization is implemented with MATLAB 2014b interfaced with GAMS 24.0. The dispatchable generating units parameters, stochastic demand and generation data are imported from CSV (comma-separated values) files to MATLAB. The dispatchable demand units and scenario parameters are setup in MATLAB from MAT files.

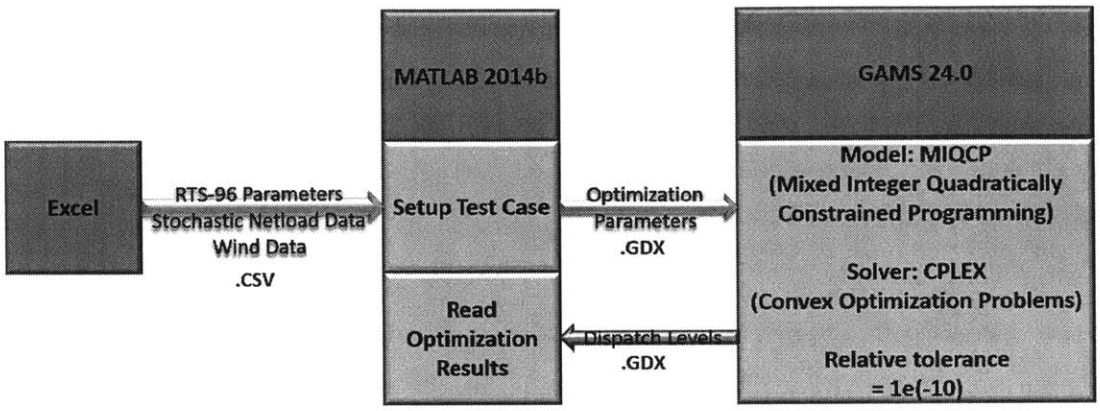

Figure 3-1: Data Flow Between MATLAB & GAMS

All data mentioned above is processed in MATLAB to construct arrays containing coefficients and parameters as in Equation (3.3) to (4.13) and write them to GDX file that can be read by GAMS. The optimization model is programmed and solved in GAMS using CPLEX as the optimization engine since both models presented in this chapter are mixed integer quadratic convex programs. A relative tolerance of 10^{-7} was chosen for all optimization problems to ensure convergence. The output of GAMS is written to GDX and read by MATLAB. Figure 3-1 shows the data flow between MATLAB and GAMS. The MATLAB and GAMS codes are listed in Appendix A.

In summary, the data importing and processing is achieved with MATLAB while the optimization is run by GAMS. It takes approximately 1000 seconds to run each optimization program on a desktop computer with Intel(R) Xeon(R) E5405 @ 2.00GHz processor.

3.6 Results & Discussion

3.6.1 Accurate Baseline

In this subsection, the two demand side management optimization programs are studied for their dispatch levels assuming an accurate baseline equal to the maximum dispatchable demand level.

Figure 3-2a and 3-2b show the dispatch levels of the social welfare and indus-

trial demand side management optimization programs respectively. The solid black line represents stochastic demand level in the social welfare model. Subtracting the stochastic generation from it gives the magenta line: the stochastic net load line in the social welfare model. The sum of dispatchable demand in red and this stochastic net load line must meet the sum of dispatchable generation to achieve power system balance. The purple line in the social welfare model represents the frontier of all the dispatchable demand units consumed at their maximum level (i.e. artificially set to the baseline level in the industrial DSM model).

The mechanics of the industrial DSM model is entirely different. The solid black line still represents the non-participating stochastic demand level. The solid yellow line adds the artificial dispatchable demand baseline to the black line. The subtraction of the stochastic generation in green from the yellow line gives the red line: the stochastic net load in the industrial DSM model. The sum of dispatchable generation in blue and the sum of dispatchable demand in purple must meet this line to achieve power system balance. Interestingly, the magenta line now represents the frontier of all the virtual generators at their maximum load reduction (i.e. virtual generation).

That the stochastic net load line in the social welfare and industrial DSM models are different is an important observation [163]. In the former, it is composed of two terms $\sum_{k=1}^{N_{DS}} \hat{P}_{DSkT} - \sum_{l=1}^{N_{GS}} \hat{P}_{GSlT}$. In the latter, it is composed of the same two terms plus a third $\sum_{k=1}^{N_{DS}} \hat{P}_{DSkT} - \sum_{l=1}^{N_{GS}} \hat{P}_{GSlT} + \sum_{j=1}^{N_{DC}} \tilde{P}_{DCjT}$. Therefore, unless the third terms systematically rejects the errors in the first two terms, it is reasonable to conclude that the stochastic netload line in the industrial DSM model is more error prone than its social welfare counterpart.

Figure 3-2 represents results from the two different approaches. Note, that as expected, the dispatchable generation and demand levels are the same for the social welfare model in Figure 3-2(a) as for the industrial model in Figure 3-2(b). It should be emphasized that instead of simple repetition of dispatch levels, the two figures demonstrate the equivalence between the two models under the condition that the industrial baseline is equal to the maximum dispatchable demand level. The numerical

simulation shows that despite the difference in optimization objective and mechanics, the two methods yield the same dispatch levels given an accurate baseline and the reconciliation between the dispatchable demand utility and virtual generation cost functions. This is consistent with the analysis in Section 3.4.2 when the proper reconciliation lead to fundamentally the same optimization problem from two different perspectives. As mentioned in Section 3.2, the dispatched generation line appears to remain relatively constant around 7000MW for much of the day. In the meantime, the dispatchable demand and virtual generation vary substantially from nearly zero to approximately 2000MW over the course of the day.

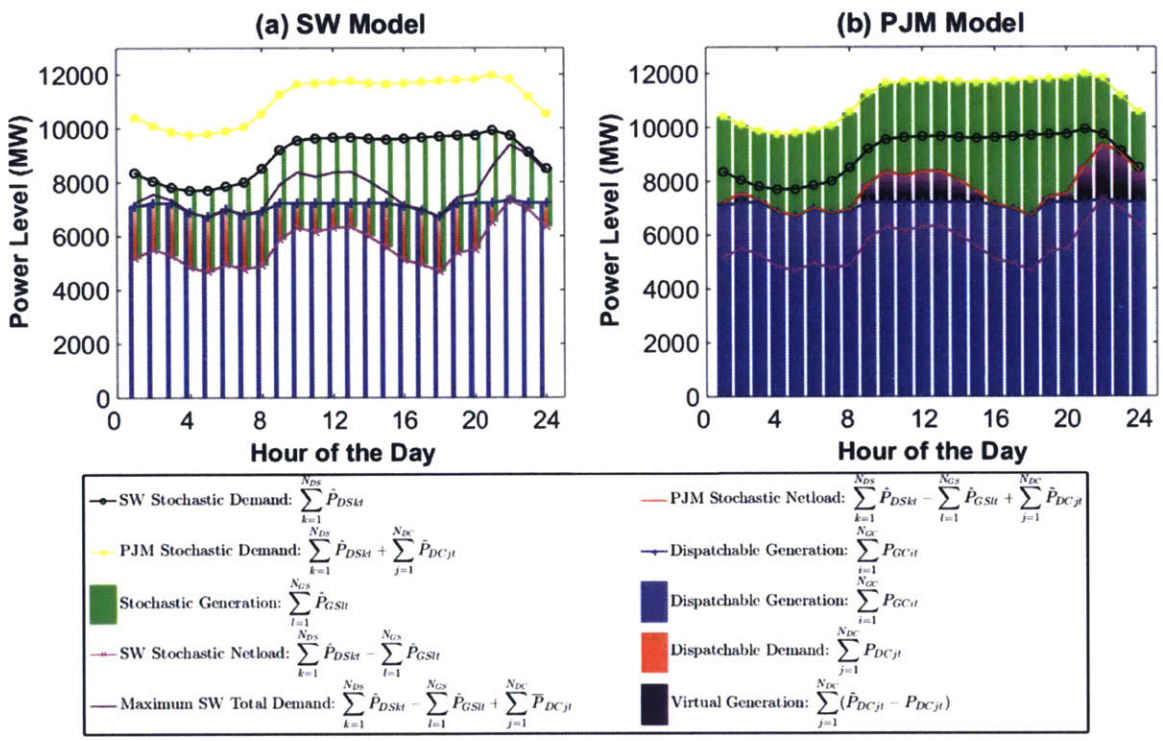

Figure 3-2: Unit Commitment Dispatch from Social Welfare & Industrial DSM with Accurate Baseline

Returning to the social welfare dispatch in Figure 3-2a, an interesting phenomenon occurs when the stochastic generation is too low or too high. For example, in Hours 22, the stochastic generation is low and the dispatchable generation must rise to meet the stochastic netload. This shows that there is a limit to the ability of social welfare demand side management helping mitigate renewable energy down-ramp events

[163]. That said, the social welfare model would still incentivize greater demand side participation in this case because it would send a long term signal that would lower the stochastic demand and stochastic net load curves. On the other hand, in Hour 18, the stochastic generation is so high that it reaches the maximum capacity of the dispatchable demand. This shows that in the case of an abundance of renewable energy, the social welfare model encourages greater demand side participation. The alternative would be to waste this energy in the form of renewable energy curtailment [163].

Industrial DSM dispatch in Figure 3-3b displays a similar behavior. The same hours can be studied for when the stochastic generation is too low or too high. In Hours 22, again the stochastic generation is too low and the virtual generation are running at maximum capacity. The dispatchable generation still needs to rise to meet power balance. As in the case of the social welfare model, the industrial DSM model is incapable of mitigating renewable energy down-ramp events although a long term signal for greater demand side management would be created. However, Hour 18 requires no virtual generation in the industrial DSM case. This means that when there is an abundance of renewable energy, there is no large incentive to expand demand side participation. These incentives instead occur in Hours 9-14 when the stochastic demand and baseline is high but not enough renewable energy exists to bring down the industrial DSM netload.

3.6.2 Inflated Baseline

The two demand side management optimization programs are now studied for their dispatch levels, social welfare values, and total system costs when the industrial DSM program is subjected to an inflated industrial baseline which is absent from the social welfare model. A 20% error was chosen to exaggerate the effects of inflated baselines.

Dispatch Levels

Figure 3-3 shows the SW and industrial dispatch levels where the baseline is 120% of the forecast. While the SW dispatch result remains the same, in the industrial dispatch, the industrial dispatchable generation (blue line) in Figure 3-3b becomes fairly constant compared to that from social welfare model in Figure 3-3a. In Hour 5 & 18, the industrial model shows that the virtual generation participate in maintaining a relatively constant dispatchable generation level. This is because the model assumes higher DSM participation than actually exists. However, the dispatched level may not always be achievable, thus requiring more subsequent control.

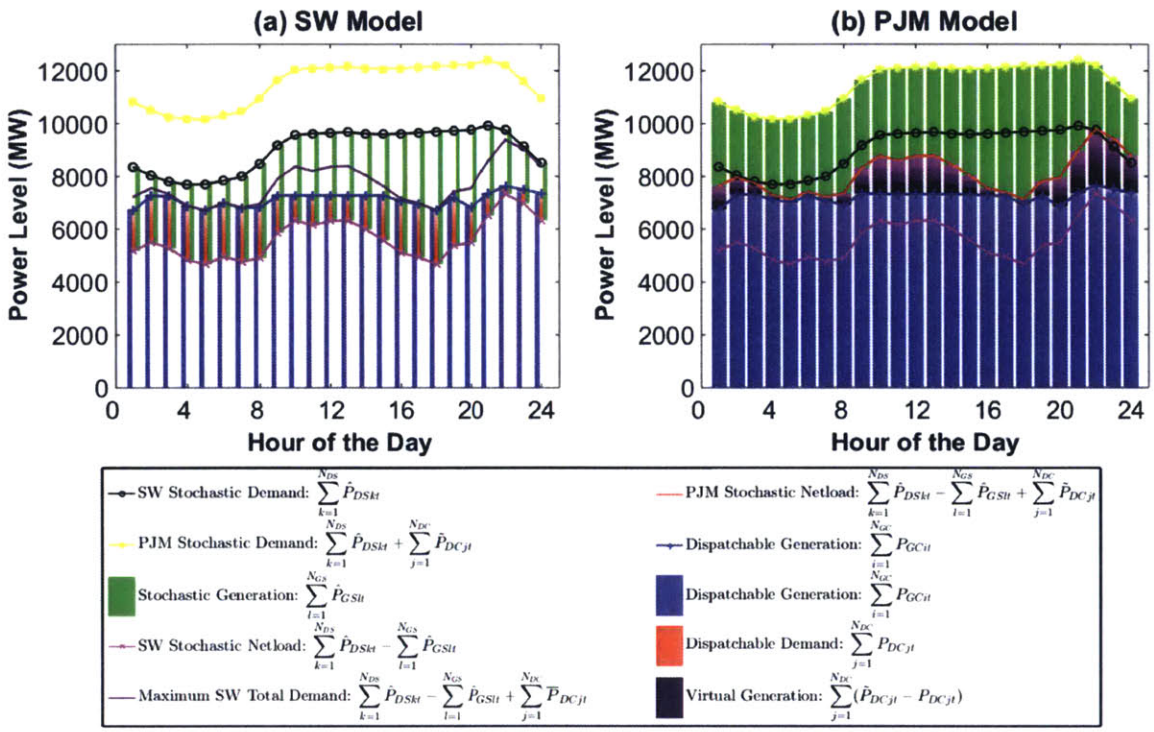

Figure 3-3: Unit Commitment Dispatch from Social Welfare & Industrial DSM with Inflated Baseline

Social Welfare

Making a rigorous and fair comparison between the two optimization programs requires borrowing the concepts from each optimization program and artificially applying into the domain of the other. Although the industrial DSM model does not

optimize social welfare, the social welfare can still be evaluated for both cases. Figure A-2 evaluates the social welfare function $\mathcal{W}$ for both simulations. As expected, the hourly social welfare value is highest in Hours 17-20 when the stochastic generation is high and the stochastic net load is low. In contrast, it is lowest in Hours 21-23 when the stochastic generation is low and the stochastic net load is high. Interestingly, and perhaps unintuitively, the industrial model with artificially high baseline results in "higher" social welfare values. Because the virtual generators are starting from the inflated baseline, their marginal costs accumulate more rapidly than if they had started from the true baseline. As a result, they end up demanding more as measured from zero. This artificially inflates the social welfare function perhaps beyond what is achievable. For example, in the case that the virtual generators are dispatched between 0 and 20% of the baseline, then they are being dispatched to demand *more* than the original load forecast or correct baseline value. This yields a higher social welfare value but does not have a basis in reality.

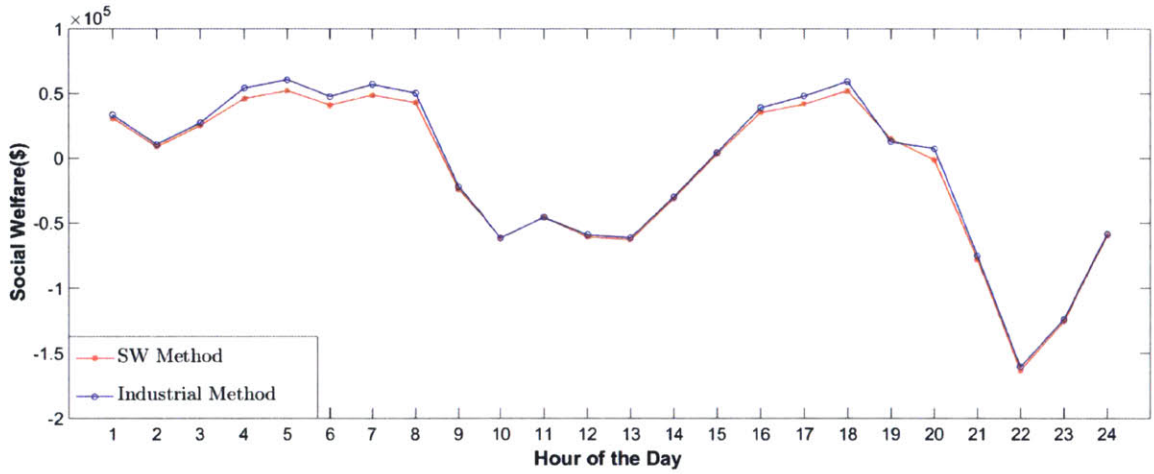

Figure 3-4: Social Welfare Values from the Social Welfare & Industrial Unit Commitment Model

System Costs

Figure 3-5 now evaluates the total system cost function in Equation (3.15) and compares the results in a similar way. While the industrial model cost is evaluated using an inflated baseline, the social welfare model evaluates the total system cost from an

error-free baseline. As expected, the cost from the industrial model is consistently higher than that from the social welfare model because it is compensating for false load reductions. The total costs for the social welfare and industrial models were $4.45 * 10^6$\$ and $5.12 * 10^6$\$ respectively. Thus, in this case the 20% error in industrial baseline lead to a 14.9% difference in the total costs.

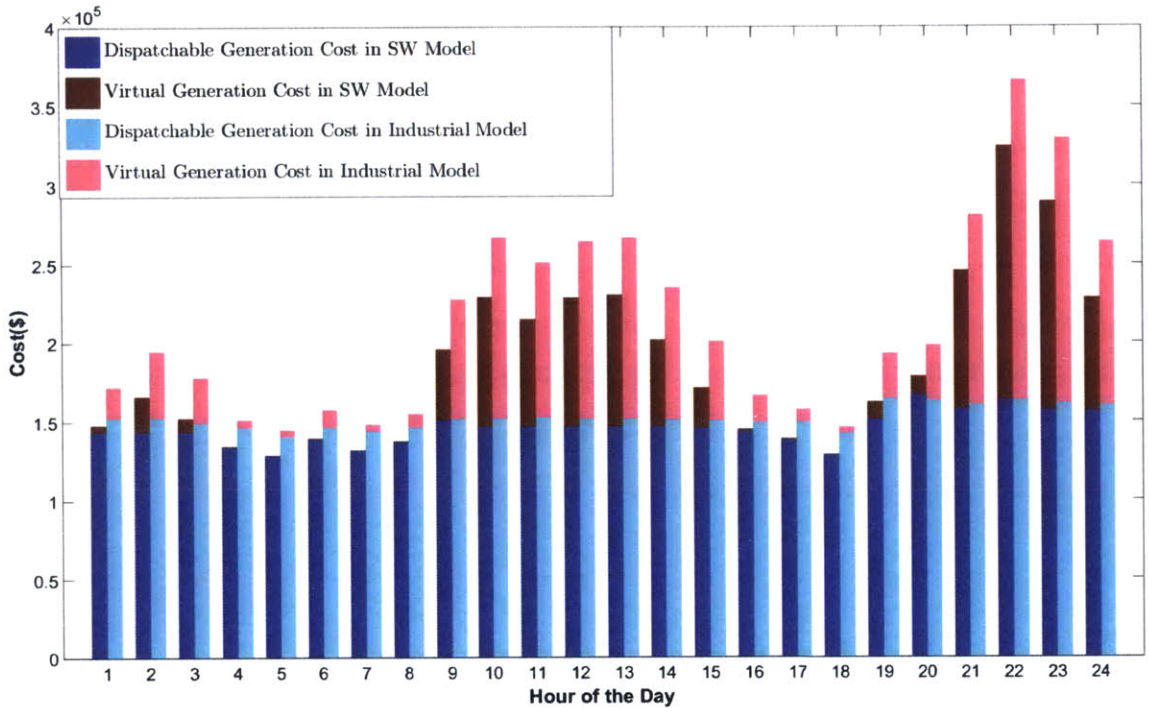

Figure 3-5: System Cost in Social Welfare & Industrial Unit Commitment DSM Models

3.7 Conclusion

The industrial & academic literature have taken divergent approaches to demand side management implementation. While academic implementations have sought to optimize social welfare, industrial implementations optimize total costs where virtual generators are compensated for their load reduction from a predefined baseline. This work has rigorously compared the two methods using the same test case. The comparison showed that while the social welfare model uses a stochastic net load composed of two terms, the industrial DSM model uses a stochastic net load composed of three

terms including an additional term for the electricity consumption baseline. It is thus more prone to error because customers have the potential to artificially inflate this baseline to gain higher financial compensation for load reduction. In the case that the baseline systematically rejects error, the two methods mitigate the stochastic net load in fundamentally the same way and incentivize same participation under various conditions of renewable energy integration and conventional demand, assuming the utility functions of dispatchable demands and cost functions of virtual generators are properly reconciled. This work has also compared the two models while introducing a 20% error in industrial electricity consumption baseline. The comparison showed that the errors in baselines lead to different dispatch levels, higher systems costs, and potentially unachievable levels of social welfare. Furthermore, the erroneous baselines is also likely to require more control activity after commitment in subsequent layers of enterprise control [1, 166, 167, 146, 147].

THIS PAGE INTENTIONALLY LEFT BLANK

Chapter 4

Impacts of Industrial Baseline Errors in Demand Side Management Enabled Enterprise Control

Chapter 3 has demonstrated that the inflation of the netload baseline forecast, used by the industrial unit commitment formulation, leads to higher and costlier day-ahead scheduling of dispatchable resources compared to the academic method. Consequently, these baseline inflation errors have to be corrected in the downstream enterprise control activities at faster time scales, increasing the control efforts and reserve requirements for the real-time market dispatch and regulation service. This chapter compares the two DSM approaches and quantifies the technical impact of industrial baseline errors in subsequent layers of control using an enterprise control methodology. The adopted enterprise control simulator encompasses three interconnected layers: a resource scheduling layer composed of a security-constrained unit commitment (SCUC), a balancing layer composed of a security-constrained economic dispatch (SCED), and a regulation layer. Baseline error is absent in the social welfare model. The simulations with the industrial model are run for different baseline error

levels. The baseline inflation is assumed to have the same effects in the day-ahead and real-time market. The resulting implications of baseline errors on power grid imbalances and regulating reserve requirements are tracked. It is concluded that with the same regulating service, the introduction of baseline error leads to additional system imbalance compared to the social welfare model results, and the imbalance amplifies itself as the baseline error increases. As a result, more regulating reserves are required to achieve the same satisfactory system performance with higher baseline error.

4.1 Introduction

The industrial and academic literature are taking divergent approaches to DSM implementation. DSM with its ability to allow customers to adjust electricity consumption in response to market signals provides additional dispatchable resources to mitigate the variable effects of renewable energy [22, 23]. Its advantages have been discussed in the context of enhancing electrical grid reliability as well as reducing system costs through peak load shaping and emergency response [17, 19, 20]. While the common approach among academic researchers is to maximize social welfare defined as the net benefits from electricity consumption and generation based on the utility of dispatchable demand [31, 32, 33], the industrial trend has been to compensate customers for load reductions from baseline electricity consumption [34, 35, 39]. Such a baseline is defined as the electricity consumption that would have occurred without DSM and is estimated from historical data from the prior year [42, 43]. Thus, dispatchable demand reductions are also treated as "virtual generators".

Previous work has demonstrated that while the net load in the academic DSM is composed of two terms, the net load in the industrial DSM is composed of three with an additional baseline term and, therefore, introduces additional forecast errors [163]. The work showed the equivalence of the two methods provided that 1) the utility function of dispatchable demand and the cost function of virtual generation are properly reconciled and 2) the industrial baseline is the same as the load forecast [163]. However, the accuracy of baseline forecast is not likely achievable, since the

load forecast is calculated a day in advance based upon sophisticated methods [44], while the baseline calculation involves much more basic formulae and is determined months in advance [45, 47]. Indeed, the customers have an implicit incentive to surreptitiously inflate the administrative baseline for greater compensation, taking advantage of greater awareness of their facilities than the regulatory agencies charged with estimating the baseline [50, 51]. Successful baseline manipulation has been shown to result in higher levels of day-ahead dispatchable resources scheduling and higher costs in the unit commitment problem. As a result, this baseline error have to be corrected in downstream enterprise control activities at faster time scales, likely requiring greater control effort and higher reserve amounts. This chapter compares the two approaches of DSM and seeks to quantify the technical impact of baseline error in subsequent control layers using an enterprise control simulator added with a dispatchable demand module. The baseline errors are simulated and the resulting implications on power grid performance are tracked, focusing on system imbalances and regulating reserve requirements. Such assessment is enabled by the recently developed enterprise control assessment method.

The enterprise control assessment method for variable energy resource induced power system imbalances has been recently developed based on the concept of enterprise control [12, 13]. It consists within a single package most of the balancing operation functionality found in traditional power systems. Previous to this development, extensive academic and industrial literature has been developed to determine the technical and economic feasibility of integrating a certain amount of variable energy resources [4, 5, 6, 7, 8, 9, 10, 11]. But most studies have one or more of the following significant methodological limitations: they are case specific [14], only address a single control function of power grid balancing operations and restricted to the timescale of the chosen function [15], or limited to statistical calculations, which are yet to be validated by simulations [16]. In contrast, this newly proposed holistic assessment method is case independent, addresses both physical as well as enterprise control processes, and is validated by a set of numerical simulations.

The remainder of this chapter develops in five sections. Section 4.2 summarizes the

highlights from the enterprise control methods, as well as the academic and industrial DSM implementation. In Section 4.3, the mathematical formulations are developed and reconciled. The text case and methodology are presented in Section 4.4. Section 4.5 presents and discusses the case study results. The chapter concludes in Section 4.6.

4.2 Background

This section summarizes the highlights from the enterprise control model, and the two DSM methods.

4.2.1 Enterprise Control

The power system enterprise model encompasses three consecutive control layers on top of the physical grid: resource scheduling layer in the form of a security-constrained unit commitment (SCUC), balancing actions in the form of a security-constrained economic dispatch (SCED) and manual actions, and regulation service in the form of automatic generation control (AGC)[12]. Each lower layer operates at a smaller timescale resulting in subsequently smaller imbalances. The SCUC uses the day-ahead net load forecast to schedule generation with a coarse time resolution. The SCED uses the available load following and ramping reserves to re-dispatch generation units in the real-time market using the short-term net load forecast. In the regulation service layer, the available regulation reserves are used to fine-tune the system balance [12].

The variable energy resources (VER) model is characterized by five parameters for systematic establishment of different integration scenarios: penetration level, capacity factor, variability, day-ahead and short-term forecast errors. The penetration level and capacity factor together determine the actual VER output. The day-ahead forecast error is used by the SCUC problem, while the short-term forecast error is an input to the SCED problem. Variability measures the changing rate of VER [12].

Readers are referred to [12] for detailed description of each control layer and the formal definitions of the five parameters listed above. References [12, 16, 168] include

the definitions of reserve types, namely load following and ramping reserves used in the real-time market, and the regulation reserve used in the regulation service.

4.2.2 Social Welfare vs Industrial DSM

The simplest form of the social welfare maximization from [156] is commonly used in academic research. Elastic demand is characterized by its utility, that is the benefit from electricity consumption, and generation is characterized by its cost [156]. The optimization determines the electricity prices and setpoints for all dispatchable resources simultaneously to maximize the net benefits [31].

Much like the social welfare model, the DSM dispatch schedule and price are jointly determined by suppliers and consumers [31] to minimize the total cost of the dispatchable and virtual generations. A curtailment service provider (CSP) represents the demand units participating in the wholesale energy market. Each CSP has an "administratively-set" electricity consumption baseline as an estimate of consumption without DSM incentives and from which load reductions are measured. Accepted load reductions are subsidized by ISO/RTO. Customers have an implicit incentive to surreptitiously inflate the administrative baseline for greater compensations, and successful baseline manipulation may cause generation relocation and inefficient price information [50].

4.3 Model Development

This section describes the SCUC & SCED mathematical models with dispatchable demand units for both DSM methods and the reconciliation between the two models.

4.3.1 Social Welfare Model

The social welfare UC optimization program with dispatchable demand has been described in detail in the prequel to this chapter [163]. In the real-time market, the SCED moves the available dispatchable generation and demand units to new

setpoints based on the short-term net load forecast. In contrast to the SCUC, the SCED problem runs at each real-time dispatch time step and determines the changes in power levels for one point at a time, and it only dispatches units determined online by SCUC, Also, the SCED does not make decisions on the on/off states. Inclusion of transmission configuration is necessary. Some input parameters depend on the current state of the system, and are calculated prior to each SCED iteration based on a full AC power flow analysis of the system [12]. The optimization goal is to maximize incremental social welfare, formulated as the first derivative of the social welfare function:

$$\Delta \mathcal{W}_t = \sum_{j=1}^{N_{DC}} \Delta \mathcal{U}_{DCjt} - \sum_{i=1}^{N_{GC}} \Delta \mathcal{C}_{GCit} \tag{4.1}$$

where

$$\Delta \mathcal{U}_{DCjt} = B_{DCj} \Delta P_{DCjt} + 2A_{DCj} P_{DCjt} \Delta P_{DCjt} \tag{4.2a}$$

$$\Delta \mathcal{C}_{GCit} = B_{GCi} \Delta P_{GCit} + 2A_{GCi} P_{GCit} \Delta P_{GCit} \tag{4.2b}$$

subject to power balance constraint in (4.3).

$$\sum_{l=1}^{N_B} (1 - \gamma_{bt})(\Delta P_{bt} - \Delta D_{bt} - \Delta \hat{D}_{bt}) = 0 \tag{4.3}$$

where

$$\Delta P_{bt} = \sum_{i=1}^{N_{GC}} M_{bi} \Delta P_{GCit}, \quad \Delta D_{bt} = \sum_{j=1}^{N_{DC}} M_{bj} \Delta P_{DCjt} \tag{4.4}$$

The incremental transmission loss factor (ITLF) γ_{bt} for bus b shows how much the total system losses change when power injection on bus b increases by a unit [169]. Line flow limits are shown in (4.5). The generation shift distribution factor (GSDF) a_{hbt} shows how much the active power flow through line h changes when injection on bus b increases by a unit [169, 170]. Additional constraints include capacity limits for dispatchable demand and generation units in (4.6 & 4.7), and ramping limits for

dispatchable demand and generation units in (4.8 & 4.9) respectively.

$$\sum_{b=1}^{N_B} a_{hbt}(\Delta P_{bt} - \Delta D_{bt} - \Delta \hat{D}_{bt}) \leq \overline{F_h} - F_{ht} \tag{4.5}$$

$$P_{DCjt} - \underline{P_{DCj}} \leq \Delta P_{DCjt} \leq \overline{P_{DCji}} - P_{DCjt} \tag{4.6}$$

$$P_{GCit} - \underline{P_{GCi}} \leq \Delta P_{GCit} \leq \overline{P_{GCi}} - P_{GCit} \tag{4.7}$$

$$\underline{R_{DCj}} * T_{ED} \leq \Delta P_{DCj} \leq \overline{R_{DCj}} * T_{ED} \tag{4.8}$$

$$\underline{R_{GCi}} * T_{ED} \leq \Delta P_{GCi} \leq \overline{R_{GCi}} * T_{ED} \tag{4.9}$$

The incorporation of ITLF into the model results in a linearization of the power balance constraint. The incorporation of GDSF into the model results in a linearization of the line flow limit constraint.

4.3.2 Industrial Model with Baseline

The industrial UC optimization program integrating dispatchable demand has been described in detail in [163]. Much like the SW model, the industrial SCED optimizes for one point of time and includes transmission losses. The optimization goal is to minimize the total incremental cost, formulated as the first derivative of the cost function:

$$\sum_{i=1}^{N_{GC}} \Delta \mathcal{C}_{GCit} + \sum_{j=1}^{N_{DC}} \Delta \mathcal{C}_{DCjt} \tag{4.10}$$

where the dispatchable generation incremental costs remain the same and

$$\Delta \mathcal{C}_{DCjt} = -\mathbb{B}_{DCj} \Delta P_{DCjt} - 2\mathbb{A}_{DCj} P_{DCjt} \Delta P_{DCjt} \tag{4.11}$$

The optimization is subject to the same power balance constraint in (4.3) and line flow limits in (4.5), capacity limits for virtual and dispatchable generation units in (4.12 & 4.7), and ramping limits for virtual and dispatchable generation units in (4.8 & 4.9) respectively.

$$(\tilde{P}_{DCjt} - P_{DCjt}) - \underline{\tilde{P}_{DCj} - P_{DCj}} \leq -\Delta P_{DCjt} \tag{4.12a}$$

$$-\Delta P_{DCjt} \leq -\overline{\tilde{P}_{DCj} - P_{DCj}} - (\tilde{P}_{DCjt} - P_{DCjt}) \tag{4.12b}$$

4.3.3 Model Reconciliation

The same model reconciliation in [163] is adopted. Namely

$$\mathbb{A}_j = -A_j, \quad \mathbb{B}_j = 2 * A_j * \tilde{P}_{DCj} + B_j \tag{4.13}$$

Table 4.1: Stochastic Demand & Stochastic Generation Characteristic Parameters in Enterprise Control Simulation

	Penetration Level	Capacity Factor	Variability	Day-Ahead Forecast Error	Short-Term Forecast Error
Load	-	-	1	0.01	0.01
Wind	0.2	1	1	0.05	0.05

4.4 Case Study

This section describes the test cases and methodology used in this chapter. The simulations consist of five scenarios that demonstrate the impact of baseline errors on system imbalances.

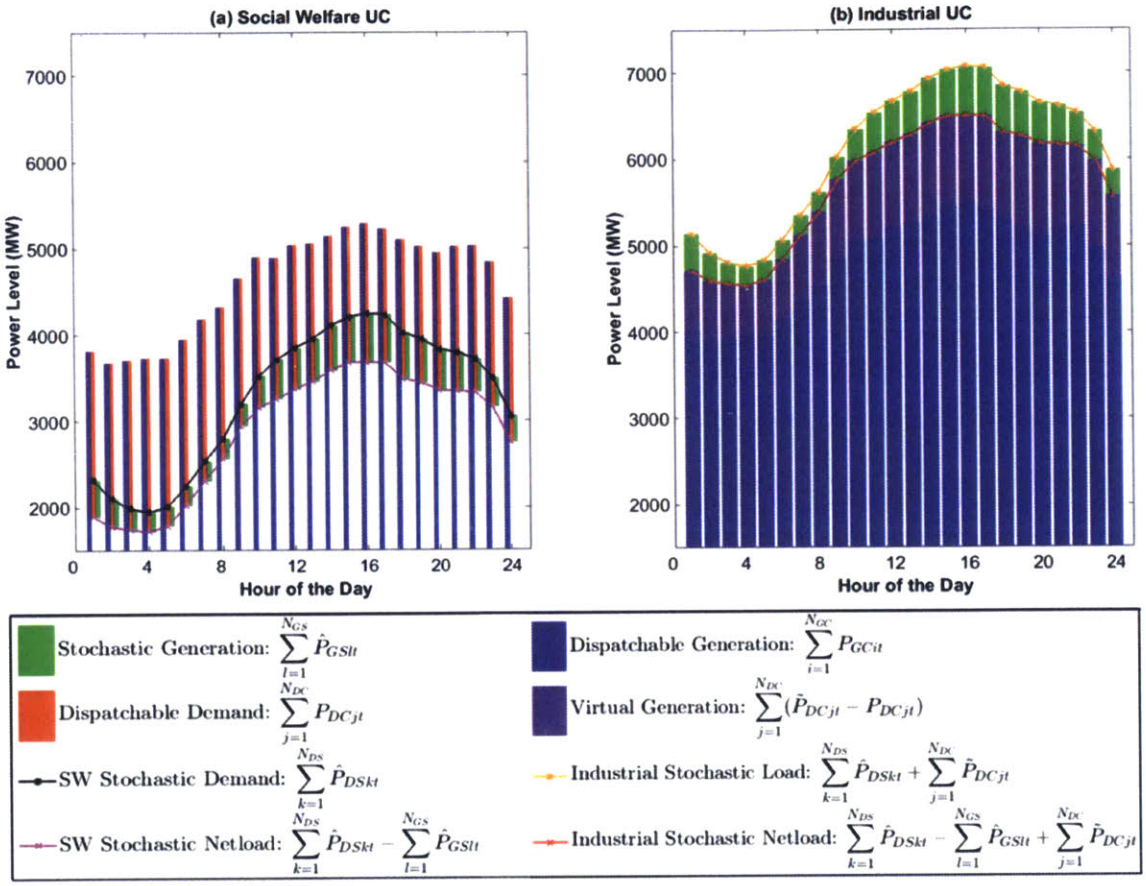

Figure 4-1: Enterprise Control SCUC Layer Dispatch from Social Welfare & Industrial DSM Model

4.4.1 Test Case & Simulation Data

Timescales

The SCUC simulation runs at the beginning of the 24 hour time span and has 1-hour time step. The SCED and regulation run over the course of the day and have time steps of 5 minutes and 1 minute respectively.

Dispatchable Generation & Dispatchable Demand

The IEEE RTS-96 (Reliability Test System-1996) is used as the physical grid configuration [171], which is consisted of 99 generators, 73 busses and 8550MW of peak load. An adequate load-following reserve is set to 20% of the peak load to allow good load-tracking in the real-time market. This ensures that the regulating service

is mostly utilized to offset the residual imbalances from the real-time market.

In this work, each aggregated dispatchable demand is assumed to occur at each bus. In the social welfare model, the minimum and maximum capacity limits of each dispatchable demand unit is assumed to be zero and 9.6% of the peak load at the corresponding bus. The impact of dispatchable demand also depends on the distribution of dispatchable units on the system buses. A random distribution may lead to heavy congestions on some transmission lines and is a topic for future investigation. The utility function coefficients for all dispatchable demand units are assumed to be equal and time-invariant. In the industrial model, an accurate baseline equals the maximum capacity of the dispatchable demand in the social welfare model. The baseline inflation error is assumed to be the same in both energy markets. Simulations are run for different baseline error levels. The startup and shutdown costs of dispatchable demand units and virtual generators have entirely different physical meanings in the social welfare and industrial DSM models and are set to zero for fairness of comparison.

Stochastic Load & Stochastic Generation

The stochastic load in the social welfare model is defined to be the load from the non-participating customers. Load and wind daily profiles are taken from Bonneville Power Administration (BPA) repositories with 5 minutes resolution [165]. The raw data are up-sampled to a 1-minute resolution using *sinc* functions to avoid distortions in the power spectrum [172]. The load and wind parameters are tabulated in Table 4.1. This work assumes that the distribution of VER capacity on the system buses is proportional to the peak loads on corresponding buses [12]. Furthermore, the VER outputs are assumed to be perfectly correlated to eliminate the effect of geographical smoothing on the reserve requirement [173].

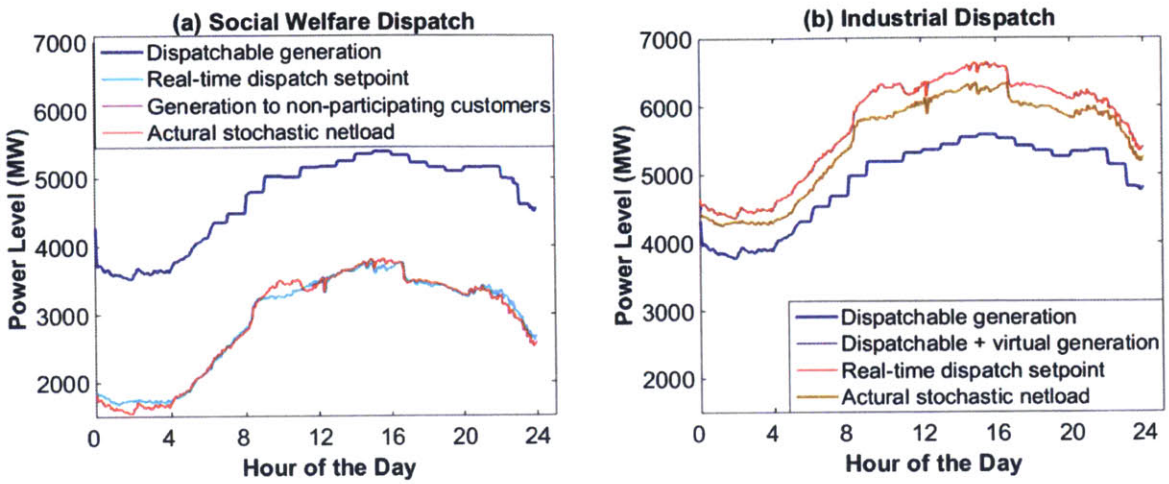

Figure 4-2: Enterprise Control SCED Layer Dispatch from Social Welfare & Industrial DSM Model

4.4.2 Computational Method

The simulator is implemented with MATLAB interfaced with GAMS. While the UC problem is carried out in GAMS using CPLEX for mixed integer quadratic constraint (MIQCP) programs, the rest of simulations including test case setup, linearized economic dispatch, regulation and power flow analysis are performed in MATLAB. One day simulation lasts 196 seconds with Inter(R) Core(TM) i7-4600 CPU @ 2.10GHz on 8.00GB RAM, showing a 20% increase in time with the addition of dispatchable demands.

4.5 Results & Discussion

This section shows the scheduling from day-ahead unit commitment and real-time economic dispatch. At various regulating reserves levels, the system imbalances are tracked for social welfare model and at different baseline errors for the industrial model.

4.5.1 Day-Ahead Dispatch Levels

Figure 4-1 compares the SCUC by both methods. Figure 4-1(a) shows the social welfare optimization. The difference between the stochastic demand from non-participating customers (solid black line) and the wind generation (green bars) gives the stochastic net load in the social welfare model (magenta line). The dispatchable generation in blue bars meets the sum of stochastic net load in magenta line and dispatchable demand in red bars. Figure 4-1(b) shows the industrial UC with a 10% baseline error. The solid orange line shows industrial stochastic demand including load from non-participating customers and baseline load from DSM participants. The subtraction of the wind generation in green bars from the orange line gives the red line: the industrial stochastic net load. It is met by the sum of dispatchable generation in blue bars and virtual generation in purple bars. In both models, ramping of dispatchable resources occurs at the first five minutes of each hour.

Comparing 4-1(a)&(b), it is observed that the baseline inflation results in erroneously high dispatchable and virtual generation. The excess dispatchable generation will be offset in real-time economic dispatch given enough load-following reserves, and otherwise further carried over to regulation layer.

4.5.2 Dispatch Levels in Real-Time

It should be emphasized that Figure 4-2 shows SCED results at 1-minute sampling rate, but has implications from SCUC and regulation layers, since SCED only dispatches units decided online by UC, and regulation participates in system balancing. For both models, the results have a sampling rate of 1 minute, and are plotted with lines instead of bars for the purpose of clarity. The relationship of subtracting wind generation from stochastic load gives the stochastic net load is straightforward, and is not demonstrated.

Figure 4-2(a) shows social welfare SCED. The magenta line shows the set-point for meeting stochastic net load, and is the net result from stochastic netload and compensation for previous imbalances. The solid blue line represents the dispatchable

generation. Subtracting the dispatchable demand consumption from this blue line gives the red line: the generation allocated to the stochastic demand from the non-participating customers. The magenta and red line coincide very five minutes at each real-time dispatch, indicating adequate load following reserves. The actual real-time net load is then represented by the solid cyan line. The deviation between the setpoint and the actual net load is mainly due to the stochastic load and wind forecast error.

Figure 4-2(b) shows the real-time dispatch of the industrial model with a 10% baseline error. The solid blue line represents the dispatchable generation. The purple line shows the sum of dispatchable and virtual generation. The solid red line represents the set-point of total generation, and is determined from the the sum short-term industrial stochastic net load forecast and the imbalance at previous dispatch. Again the red and purple line meet at dispatch time points, indicating adequate load-following reserves. Now interestingly comes the actual industrial stochastic net load represented by the brown line with no baseline error. The huge deviation between the set-point and the actual net load is mostly due to the baseline error, in addition to the stochastic load and wind forecast error.

4.5.3 System Imbalance vs. Regulating Reserves

In Figure 4-3, each curve plots the averaged absolute system imbalance against the regulating reserves where both quantities are normalized against the peak load. The absolute imbalance is summed over all buses to represent the total system imbalance at each specific time point. This quantity is then averaged at a one-minute sample rate over the day to evaluate the system performance. As expected, better system performance is observed at greater regulating reserve amount for all scenarios. The blue line shows the system imbalance from social welfare model, and in other words, no baseline errors. The system has a 0.68% averaged imbalance without regulating services, and drops below 0.02% after the reserve reaches 5% of peak load. The orange, yellow, purple, and green line represents industrial model with 1%, 2%, 5%, and 10% respectively. At zero regulating service, they have 0.74%, 0.8%, 1.4%, and 2.9% averaged system imbalance, which drops below 0.02% after the regulating reserve is

increased to 6%, 6%, 8%, and 11% respectively.

Generally speaking, higher system imbalances are associated with larger baseline errors. In the social welfare model where the dispatch is free from baseline errors, the system is still subject to load and wind forecast errors. In the industrial model, the introduction of baseline forecast exacerbates the overall forecast error. The imbalance in the case with 1% baseline error is comparable to that in the social welfare model when the error is relatively small compared to the other forecast errors. The imbalance increases rapidly as the baseline error is raised to 5% and 10%. Unfortunately as explained in the introduction, the baseline forecast is likely to have low accuracy and the cases with high imbalance are likely to occur.

4.6 Conclusion

This chapter compares the academic and industrial DSM implementations using a recently developed enterprise control model added with a dispatchable demand module. The baseline introduces one more forecast quantity and therefore higher forecast errors to the industrial model. The baseline errors result in erroneously high dispatch levels in both the day-ahead and real-time markets, and the error is then carried over to the regulation layer. Higher system imbalances are induced by higher baseline errors, which requires greater regulation reserves amount to achieve the same satisfactory system performance.

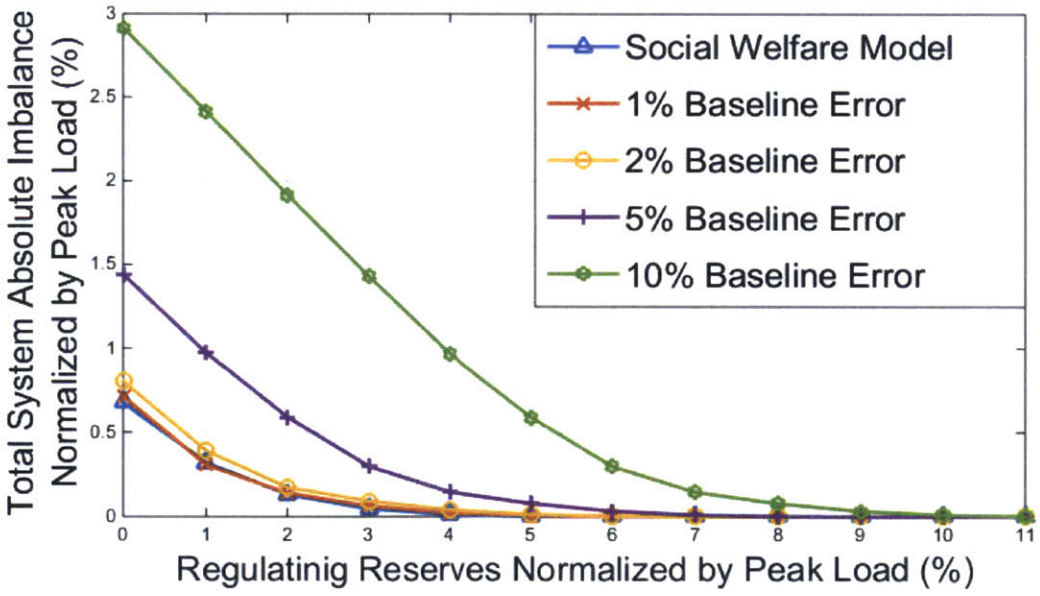

Figure 4-3: System Imbalances vs. Regulating Reserves

THIS PAGE INTENTIONALLY LEFT BLANK

Chapter 5

Conclusions & Recommendations

5.1 Conclusions

This thesis is devoted to the DSM in the context of enterprise control assessment. This work first contrasted the existing renewable energy integration study limitations to a holistic assessment framework and argued the necessity of incorporating DSM for VER intermittency mitigation. The industrial & academic literature have taken divergent approaches to demand side management implementation. While academic implementations have sought to optimize social welfare, industrial implementations optimize total costs where virtual generators are compensated for their load reduction from a predefined baseline. This work rigorously compared the two methods analytically and numerically in a day-ahead wholesale market using the same mathematical formalism and system configuration. The comparison showed that the industrial net-load introduces an additional term of baseline consumption, and the two models are equivalent given proper cost and utility reconciliation and accurate baselines. However, a baseline artificially inflated by customers occurs more often in reality, and lead to higher and costlier dispatchable resources scheduling and unachievable social welfare compared to the academic method. This thesis then proceeds to compare the two DSM approaches and quantifies the technical impact of industrial baseline errors in subsequent layers of control using an enterprise control methodology. The simulator is implemented by MATLAB interfaced with GAMS, and incorporates power

flow analysis and three interconnected control layers: a resource scheduling layer, a balancing layer and a regulation layer. The day-ahead wholesale market adopts a unit commitment problem and the real-time wholesale market adopts an economic dispatch (ED) problem on the timescale of minutes. While baseline error is absent in the social welfare model, the industrial model is simulated with different baseline levels, assuming the baseline inflation has the same effects in the day-ahead and real-time market. The resulting implications of baseline errors on power grid imbalances and regulating reserve requirements are tracked. It is concluded that with the same regulating service, the introduction of baseline error leads to additional system imbalance compared to the social welfare model results, and the imbalance amplifies itself as the baseline error increases. As a result, more regulating reserves are required to achieve the same satisfactory system performance with higher baseline error.

In summary, the industrial DSM baseline inflation brings about higher and costlier dispatch in day-ahead wholesale market and higher reserve requirements and system imbalances in subsequent control layers, namely the real-time market regulating service.

5.2 Recommendations

The immediate next stage of this work should be the modeling of time-variant dispatchable demand unit capacities and time-variant virtual generation cost functions. It is also suggested that historical or survey data be used for the ramping rate limits of dispatchable demand units.

An interesting topic for future investigation is the impact of distribution of demand units on the system buses. A random distribution may lead to heavy congestion on some transmission lines and the result can be used for designing optimal system topology.

Another significant topic is the curtailment of the renewable energy. A module with renewable energy harvest devices such as wind turbines can be added to the enterprise control to expand the study scope. The incorporation of power connection

to the bulk grid can provide valuable information on the feasibility of integrating renewable energy at high penetration levels.

THIS PAGE INTENTIONALLY LEFT BLANK

Bibliography

[1] A. M. Farid, B. Jiang, A. Muzhikyan, and K. Youcef-Toumi, "The Need for Holistic Enterprise Control Assessment Methods for the Future Electricity Grid," *under review: Renewable & Sustainable Energy Reviews*, vol. 1, no. 1, pp. 1–8, 2014.

[2] C. Grigg, P. Wong, P. Albrecht, R. Allan, M. Bhavaraju, R. Billinton, Q. Chen, C. Fong, S. Haddad, S. Kuruganty, W. Li, R. Mukerji, D. Patton, N. Rau, D. Reppen, A. Schneider, M. Shahidehpour, and C. Singh, "The IEEE Reliability Test System-1996. A report prepared by the Reliability Test System Task Force of the Application of Probability Methods Subcommittee," *IEEE Transactions on Power Systems*, vol. 14, no. 3, pp. 1010–1020, 1999.

[3] U.S. Energy Information Administration, "Short-Term Energy Outlook," November 2014.

[4] K. Dykes, "Integration of Wind into the Electricity System," MIT, Cambridge, Tech. Rep., 2010.

[5] E. A. DeMeo, W. Grant, M. R. Milligan, and M. J. Schuerger, "Wind plant integration: Costs, Status, and Issues," *Power and Energy Magazine, IEEE*, vol. 3, no. 6, pp. 38–46, 2005.

[6] J. Smith, M. Milligan, E. DeMeo, and B. Parsons, "Utility Wind Integration and Operating Impact State of the Art," *IEEE Transactions on Power Systems*, vol. 22, no. 3, pp. 900–908, Aug 2007.

[7] A. M. Farid and A. Muzhikyan, "The Need for Holistic Assessment Methods for the Future Electricity Grid," in *GCC Power 2013 Conference & Exhibition*, Abu Dhabi, UAE, 2013, pp. 1–13.

[8] K. De Vos and J. Driesen, "Dynamic operating reserve strategies for wind power integration," *IET Renewable Power Generation*, vol. 8, no. 6, pp. 598–610, 2014.

[9] Z. Zhou and A. Botterud, "Dynamic Scheduling of Operating Reserves in Co-Optimized Electricity Markets With Wind Power," *IEEE Trans. Power Syst.*, vol. 29, no. 1, pp. 160–171, 2014.

[10] A. Ahmadi-Khatir, A. J. Conejo, and R. Cherkaoui, "Multi-Area Unit Scheduling and Reserve Allocation Under Wind Power Uncertainty," *IEEE Trans. Power Syst.*, vol. 29, no. 4, pp. 1701–1710, 2014.

[11] K. Bruninx and E. Delarue, "A Statistical Description of the Error on Wind Power Forecasts for Probabilistic Reserve Sizing," *IEEE Trans. Sustain. Energy*, vol. 5, no. 3, pp. 995–1002, 2014.

[12] A. Muzhikyan, A. M. Farid, and K. Youcef-Toumi, "An Enterprise Control Assessment Method for Variable Energy Resource Induced Power System Imbalances. Part 1: Methodology," *IEEE Trans. Ind. Electron., to be published.*

[13] ——, "An Enterprise Control Assessment Method for Variable Energy Resource Induced Power System Imbalances. Part 2: Results," *IEEE Transactions on Industrial Electronics*, vol. 1, no. 1, pp. 1–8, 2014.

[14] A. Robitaille, I. Kamwa, A. Oussedik, M. de Montigny, N. Menemenlis, M. Huneault, A. Forcione, R. Mailhot, J. Bourret, and L. Bernier, "Preliminary Impacts of Wind Power Integration in the Hydro-Quebec System," *Wind Engineering*, vol. 36, no. 1, pp. 35–52, Feb. 2012.

[15] D. A. Halamay, T. K. A. Brekken, A. Simmons, and S. McArthur, "Reserve Requirement Impacts of Large-Scale Integration of Wind, Solar, and Ocean Wave Power Generation," *Sustainable Energy, IEEE Transactions on*, vol. 2, no. 3, pp. 321–328, 2011.

[16] E. Ela, B. Kirby, E. Lannoye, M. Milligan, D. Flynn, B. Zavadil, and M. O'Malley, "Evolution of operating reserve determination in wind power integration studies," in *Power and Energy Society General Meeting, 2010 IEEE*, 2010, pp. 1–8.

[17] D. Kirschen, "Demand-Side View of Electricity Markets," *IEEE Transactions on Power Systems*, vol. 18, no. 2, pp. 520–527, May 2003.

[18] D. P. Chassin and Pacific Northwest National Laboratory, "How Demand Response Can Mitigate Renewable Intermittency," ser. 4th International Conference on Integration of Renewable and Distributed Energy Resources. IEEE, December 2000.

[19] L. Chen, N. Li, L. Jiang, and S. H. Low, "Optimal Demand Response: Problem Formulation and Deterministic Case," *Control and Optimization Methods for Electric Smart Grids*, vol. 3, pp. 63–85, 2012.

[20] G. Strbac, "Demand side management: Benefits and challenges," *Energy Policy*, vol. 36, no. 12, pp. 4419–4426, 2008.

[21] F. M. Andersen, S. G. Jensen, H. V. Larsen, P. Meibom, H. Ravn, K. Skytte, and M. Togeby, "Analyses of Demand Response in Denmark," Tech. Rep. October, Oct 2006.

[22] C. W. Gellings, "The Concept of Demand-Side Management for Electric Utilities," in *Proceedings of the IEEE*, vol. 73, no. 10, October 1985, pp. 1468–1470.

[23] P. Palensky and D. Dietrich, "Demand Side Management: Demand Response, Intelligent Energy Systems, and Smart Loads," *IEEE Transactions on Industrial Informatics*, vol. 7, no. 3, pp. 381–388, Aug 2011.

[24] J. N. Sheen, "Economic profitability analysis of demand side management program," *Energy Conversion and Management*, vol. 46, no. 18 - 19, pp. 2919 – 2935, 2005.

[25] U.S. Department of Energy, "Benefits of Demand Response in Electricity Markets and Recommendations for Achieving Them: A Report to the United States Congress Pursuant to Section 1253 of the Energy Policy Act of 2005," Tech. Rep. February, 2006.

[26] R. Walawalkar, S. Blumsack, J. Apt, and S. Fernands, "An Economic Welfare Analysis of Demand Response in the PJM Electricity Market," *Energy Policy*, vol. 36, no. 10, pp. 3692 – 3702, Oct 2008.

[27] K. Spees and L. B. Lave, "Demand response and electricity market efficiency," *The Electricity Journal*, vol. 20, no. 3, pp. 69–85, 2007.

[28] S. Neumann, F. Sioshansi, A. Vojdani, and G. Yee, "How to get more response from demand response," *The Electricity Journal*, vol. 19, no. 8, pp. 24–31, 2006.

[29] A. Zibelman and E. N. Krapels, "Deployment of demand response as a real-time resource in organized markets."

[30] J. Wu, X. Guan, F. Gao, and G. Sun, "Social Welfare Maximization Auction for Electricity Markets with Elastic Demand," in *7th World Congress on Intelligent Control and Automation, 2008. WCICA 2008*, ser. Proceedings of the World Congress on Intelligent Control and Automation (WCICA). Institute of Electrical and Electronics Engineers Inc., June 2008, pp. 7157–7162.

[31] K. Matsumoto, Y. Takamuki, N. Mori, and M. Kitayama, "An interactive approach to demand side management based on utility functions," in *International Conference on Electric Utility Deregulation and Restructuring and Power Technologies, 2000.*, 2000, pp. 147–150.

[32] L. Na, L. Chen, and S. H. Low, "Optimal demand response based on utility maximization in power networks," in *2011 IEEE Power and Energy Society General Meeting*, ser. IEEE Power and Energy Society General Meeting. IEEE Computer Society, July 2011, pp. 1–8.

[33] M. Roozbehani, M. Dahleh, and S. Mitter, "On the Stability of Wholesale Electricity Markets under Real-Time Pricing," in *2010 49th IEEE Conference on Decision and Control*, December 2010, pp. 1911–1918.

[34] FERC, "Final Rule, Order 719, Wholesale Competition in Regions with Organized Electric Markets," FERC, Tech. Rep., 2008.

[35] R. Walawalkar, S. Fernands, N. Thakur, and K. R. Chevva, "Evolution and current status of demand response (DR) in electricity markets: Insights from PJM and NYISO," *Energy*, vol. 35, no. 4, pp. 1553 – 1560, 2010.

[36] FERC, "2012 Assessment of Demand Response and Advanced Metering," FERC, Tech. Rep., 2012.

[37] P. Cappers, C. Goldman, and D. Kathan, "Demand Response in U.S. Electricity Markets: Empirical Evidence," *Energy*, vol. 35, no. 4, pp. 1526 – 1535, 2010.

[38] J. Torriti, M. G. Hassan, and M. Leach, "Demand response experience in Europe: Policies, programmes and implementation," *Energy*, vol. 35, no. 4, pp. 1575–1583, 2010.

[39] M. H. Albadi and E. F. El-Saadany, "A summary of demand response in electricity markets," *Electric Power Systems Research*, vol. 78, no. 11, pp. 1989 – 1996, 2008.

[40] H. Zhong, L. Xie, and Q. Xia, "Coupon Incentive-Based Demand Response: Theory and Case Study," in *IEEE Transactions on Power Systems*, 2013.

[41] K. Herter and S. Wayland, "Residential response to critical-peak pricing of electricity: California evidence," *Energy*, vol. 35, no. 4, pp. 1561 – 1567, 2010.

[42] N. Ruiz, I. Cobelo, and J. Oyarzabal, "A Direct Load Control Model for Virtual Power Plant Management," *IEEE Transactions on Power Systems*, vol. 24, no. 2, pp. 959–966, May 2009.

[43] E. Karangelos and F. Bouffard, "Towards Full Integration of Demand-Side Resources in Joint Forward Energy/Reserve Electricity Markets," *IEEE Transactions on Power Systems*, vol. 27, no. 1, pp. 280–289, Feb 2012.

[44] E. Almeshaiel and H. Soltan, "A Methodology for Electric Power Load Forecasting," *Alexandria Engineering Journal*, vol. 50, pp. 137–144, June 2011.

[45] PJM State & Member Training Dept., "PJM Demand Side Response," 2011.

[46] EnerNOC, "The Demand Response Baseline," Tech. Rep., 2009.

[47] K. Coughlin, M. A. Piette, C. Goldman, and S. Kiliccote, "Estimating Demand Response Load Impacts: Evaluation of Baseline Load Models for Non Residential Buildings in California," January 2008.

[48] KEMA, "PJM Empirical Analysis of Demand Response Baseline Methods," Tech. Rep., April 2011.

[49] M. L. Goldberg, G. K. Agnew, and D. Kema, "Measurement and Verification for Demand Response," Tech. Rep., February 2013.

[50] H.-p. Chao, "Demand response in wholesale electricity markets: the choice of customer baseline," *Journal of Regulatory Economics*, vol. 39, no. 1, pp. 68–88, Nov 2011.

[51] J. Bushnell, B. F. Hobbs, and F. A. Wolak, "When it comes to demand response, is FERC its own worst enemy?" *The Electricity Journal*, vol. 22, no. 8, pp. 9–18, 2009.

[52] NYISO, "Wholesale vs.Retail Electricity." [Online]. Available: http://www.nyiso.com/public/about_nyiso/understanding_the_markets/wholesale_retail/index.jsp

[53] PJM, "PJM Markets & Operations Demand Response." [Online]. Available: http://www.pjm.com/markets-and-operations/demand-response.aspx

[54] NBSO, "Maritimes Area Wind Integration Study," Tech. Rep. August, 2005.

[55] GE Energy, D. V. Zandt, L. Freeman, G. Zhi, R. Piwko, G. Jordan, and N. Miller, "Ontario Wind Integration Study," Tech. Rep., 2006.

[56] P. Meibom, Risoe National Laboratory, R. Barth, H. Brand, H. Bernhard, D. Swider, and H. Ravn, "Final Report for All Island Grid Study Work-stream 2(b): Wind Variability Management Studies," Tech. Rep. July, 2007.

[57] F. Rodriguez-Bobada, A. R. Rodrigues, A. Cena, and E. Giraut, "Study of wind energy penetration in the Iberian peninsula," Tech. Rep., 2006.

[58] DENA, "Energy Management Planning for the Integration of Wind Energy into the Grid in Germany , Onshore and Offshore by 2020," Tech. Rep. February, 2005.

[59] B. Hoflich, J. P. Molly, B. Neddermann, T. Schorer, D. Callies, K. Knorr, K. Rohrig, Y.-M. Sant-Drenan, U. Bachmann, R. Bauer, A. Konnemann, J. Muller, H. Radtke, I. August, E. Grebe, S. Groninger, C. Neumann, J. Runge, H. Abele, S. Jung, V. Schroth, O. Sener, S. Bopp, Y. Nguegan, M. Schmale, C. Siebels, W. Winter, F. Borggrefe, K. Grave, D. Lindenberger, C. Merz, M. Nicolosi, A. Nusler, J. Richter, M. Paulus, H. Samisch, J. Schwill, I. Stadler, J. Dobschinski, S. Faulstich, M. Puchta, and J. Sievers, "DENA Grid Study II: Integration of Renewable Energy Sources in the German Power Supply Systems from 2015-2020 with an Outlook to 2025," German Energy Agency, Berlin, Germany, Tech. Rep., 2010.

[60] B. C. Ummels, "Power System Operation with Large-Scale Wind Power in Liberalised Environments," Ph.D. dissertation, Technical University of Delft, 2009.

[61] U. Axelsson, R. Murray, V. Neimane, and ELFORSK, "4000 MW wind power in Sweden Impact on regulation and reserve requirements," Tech. Rep., 2005.

[62] J. Bertsh, C. Growitsch, S. Lorenczik, and S. Nagl, "Flexibility options in European electricity markets in high RES-E scenarios Study on behalf of the International Energy Agency (IEA)," Institute of Energy Economics, Cologne, Germany, Tech. Rep. October, 2012.

[63] EWIS, "European Wind Integration Study (EWIS) Towards A Successful Integration into European Electricity Grids Appendix," ENTSO-E, Brussels, Belgium, Tech. Rep., 2010.

[64] F. V. Hulle, J. O. Tande, L. Warland, M. Korpas, P. Meibom, P. Sorensen, P. E. Morthorst, N. Cutululis, G. Giebel, H. Larsen, A. Woyte, G. Dooms, P.-A. Mali, A. Delwart, F. Verheij, C. Kleinschmidt, N. Moldovan, H. Holttinen, B. Lemstrom, S. Uski-Joutsenvuo, P. Gardner, G. van der Toorn, J. McLean, S. Cox, K. Purchala, S. Wagemans, A. Tiedemann, P. Kreutzkamp, C. Srikandam, and J. Volker, "Tradewind Integrating Wind – Developing Europe's power market for the large-scale integration of wind power," European Wind Energy Association, Fredericia, DK, Tech. Rep., 2009.

[65] G. Strbac, A. Shakoor, M. Black, D. Pudjianto, and T. Bopp, "Impact of wind generation on the operation and development of the UK electricity systems," *Electric Power Systems Research*, vol. 77, pp. 1214–1227, Jul. 2007.

[66] I. Norheim, E. Lindgren, S. Uski, P. Sorensen, C. Jauch, and WILMAR, "WILMAR WP5-Deliverable D5.1 System stability analysis," Tech. Rep., 2005.

[67] EnerNex, "Final Report Avista Corporation Wind Integration Study," Tech. Rep., 2007.

[68] T. Mason, T. Curry, M. Hong, B. Joe, S. Olson, M. Sprouse, and D. Wilson, "SOLAR PHOTOVOLTAIC (PV) INTEGRATION COST STUDY," Black & Veatch, Overland Park, Kansas, Tech. Rep. 174880, 2012.

[69] S. Venkataraman, G. Jordan, R. Piwko, L. Freeman, U. Helman, C. Loutan, G. Rosenblum, J. Xie, H. Zhou, and M. Kuo, "Integration of Renewable Resources: Operational Requirements and Generation Fleet Capability at 20% RPS," Califorina-Independent System Operator, Tech. Rep., 2010.

[70] EnerNex, "EASTERN WIND INTEGRATION AND TRANSMISSION STUDY," Tech. Rep. January, 2010.

[71] GE Energy, "Final Report Analysis of Wind Generation Impact on ERCOT Ancillary Services Requirements," GE Energy for Electric Reliability Council of Texas, Tech. Rep., 2008.

[72] University of Hawaii, "Oahu Wind Integration Study," University of Hawaii, Hawaii Natural Energy Institute, School of Ocean and Earth Science and Technology, Oahu, HA, Tech. Rep. February, 2011.

[73] B. Johnson, J. Lindsay, K. Myers, P. Woods, and C. Yourkowski, "Solar Integration Study Report," Idaho Power, Tech. Rep. June, 2014.

[74] D. Savage, "Final Report - 2006 Minnesota Wind Integration Study Volume I," EnerNex Corporation, Knoxville, TN, Tech. Rep., 2006.

[75] EnerNex and NREL, "Nebraska Statewide Wind Integration Study," Tech. Rep. March, 2010.

[76] GE Energy and GE-Energy, "New England Wind Integration Study," GE Energy, Schenectady, New York, Tech. Rep. May, 2010.

[77] E. Shlatz, L. Frantzis, T. McClive, G. Karlson, D. Acharya, S. Lu, P. Etingov, R. Diao, J. Ma, N. Samaan, V. Chadliev, M. Smart, R. Salgo, R. Sorensen, B. Allen, B. Idelchik, A. Ellis, J. Stein, C. Hanson, Y. V. Makarov, X. Guo, R. P. Hafen, C. Jin, and H. Kirkham, "Large-Scale PV Integration Study," Navigant Consulting, Las Vegas, NV, USA, Tech. Rep., 2011.

[78] R. Piwko, X. Bai, K. Clark, G. Jordan, N. Miller, and J. Zimberlin, "The Effects of Integrating Wind Power on Transmission System Planning, Reliability and Operations," GE Energy, Schnectady, New York, Tech. Rep., 2005.

[79] PACIFICORP, "Project Method for 2010 Wind Integration Cost Study," Tech. Rep., 2010.

[80] GE Energy, "PJM Renewable Integration Study (PRIS) Project Review (Task 3a)," 2013.

[81] Charles River Associates, "SPP WITF Wind Integration Study," Charles River Associates, Boston, MA, Tech. Rep., 2010.

[82] GE Energy, "WESTERN WIND AND SOLAR INTEGRATION STUDY," Tech. Rep. May, 2010.

[83] D. Lew, G. Brinkman, E. Ibanez, A. Florita, M. Heaney, B. Hodge, M. Hummon, G. Stark, and J. King, "The Western Wind and Solar Integration Study Phase 2," Tech. Rep. September, 2013.

[84] H. Holttinen, M. Milligan, B. Kirby, T. Acker, V. Neimane, and T. Molinski, "Using Standard Deviation as a Measure of Increased Operational Reserve Requirement for Wind Power," *Wind Engineering*, vol. 32, no. 4, pp. 355–377, 2008. [Online]. Available: citeulike-article-id:8373954http://dx.doi.org/10.1260/0309-524X.32.4.355

[85] A. Robitaille, I. Kamwa, A. Oussedik, M. de Montigny, N. Menemenlis, M. Huneault, A. Forcione, R. Mailhot, J. Bourret, and L. Bernier, "Preliminary Impacts of Wind Power Integration in the Hydro-Quebec System," *Wind Engineering*, vol. 36, no. 1, pp. 35–52, Feb. 2012. [Online]. Available: http://dx.doi.org/10.1260/0309-524X.36.1.35

[86] C. W. Hansen and A. D. Papalexopoulos, "Operational Impact and Cost Analysis of Increasing Wind Generation in the Island of Crete," *Systems Journal, IEEE*, vol. 6, no. 2, pp. 287–295, 2012.

[87] NERC, "Reliability Standards for the Bulk Electric Systems of North America," NERC–North American Electric Reliability Corporation, Tech. Rep., 2012. [Online]. Available: http://www.nerc.com/files/Reliability_Standards_Complete_Set_1Dec08.pdf

[88] T. Aigner, S. Jaehnert, G. L. Doorman, and T. Gjengedal, "The Effect of Large-Scale Wind Power on System Balancing in Northern Europe," *Sustainable Energy, IEEE Transactions on*, vol. 3, no. 4, pp. 751–759, 2012.

[89] B. C. Ummels, M. Gibescu, E. Pelgrum, W. L. Kling, and A. J. Brand, "Impacts of Wind Power on Thermal Generation Unit Commitment and Dispatch," *IIEEE Transactions on Energy Conversion*, vol. 22, no. 1, pp. 44–51, 2007. [Online]. Available: http://dx.doi.org/10.1109/TEC.2006.889616http://ieeexplore.ieee.org/lpdocs/epic03/wrapper.htm?arnumber=4106021

[90] D. A. Halamay, T. K. A. Brekken, A. Simmons, and S. McArthur, "Reserve Requirement Impacts of Large-Scale Integration of Wind, Solar, and Ocean Wave Power Generation," *Sustainable Energy, IEEE Transactions on*, vol. 2, no. 3, pp. 321–328, 2011.

[91] M. H. Albadi and E. F. El-Saadany, "Comparative study on impacts of wind profiles on thermal units scheduling costs," *Renewable Power Generation, IET*, vol. 5, no. 1, pp. 26–35, 2011.

[92] E. Ela, B. Kirby, E. Lannoye, M. Milligan, D. Flynn, B. Zavadil, and M. O'Malley, "Evolution of operating reserve determination in wind power integration studies," in *Power and Energy Society General Meeting, 2010 IEEE*, 2010, pp. 1–8.

[93] E. Ela, M. Milligan, B. Parsons, D. Lew, and D. Corbus, "The evolution of wind power integration studies: Past, present, and future," pp. 1–8, 2009.

[94] H. Holttinen, M. O. Malley, J. Dillon, and D. Flynn, "Recommendations for Wind Integration Studies – IEA Task 25," International Energy Agency, Helsinki, Tech. Rep., 2012.

[95] H. Holttinen, A. Orths, H. Abilgaard, F. van Hulle, J. Kiviluoma, B. Lange, M. O'Malley, D. Flynn, A. Keane, J. Dillon, E. M. Carlini, J. O. Tande, A. Estanquiro, E. G. Lazaro, L. Soder, M. Milligan, C. Smith, and C. Clark, "IEA Wind Export Group Report on Recommended Practices Wind Integration Studies," International Energy Agency, Paris, France, Tech. Rep., 2013.

[96] A. S. Brouwer, M. van den Broek, A. Seebregts, and A. Faaij, "Impacts of large-scale Intermittent Renewable Energy Sources on electricity systems , and how these can be modeled," *Renewable and Sustainable Energy Reviews*, vol. 33, pp. 443–466, 2014.

[97] R. Billinton and G. Bai, "Generating capacity adequacy associated with wind energy," *Energy Conversion, IEEE Transactions on*, vol. 19, no. 3, pp. 641–646, 2004.

[98] P. J. Luickx, E. D. Delarue, and W. D. D'haeseleer, "Effect of the generation mix on wind power introduction," *Renewable Power Generation, IET*, vol. 3, no. 3, pp. 267–278, 2009.

[99] Y. V. Makarov, P. V. Etingov, J. Ma, Z. Huang, and K. Subbarao, "Incorporating uncertainty of wind power generation forecast into power system operation, dispatch, and unit commitment procedures," *IEEE Transactions on Sustainable Energy*, vol. 2, no. 4, pp. 433–442, 2011. [Online]. Available: http://dx.doi.org/10.1109/TSTE.2011.2159254

[100] Y. V. Makarov, S. Lu, N. Samaan, Z. Huang, K. Subbarao, P. V. Etingov, J. Ma, R. P. Hafen, R. Diao, and N. Lu, "Integration of uncertainty information into power system operations BT - 2011 IEEE PES General Meeting: The Electrification of Transportation and the Grid of the Future, July 24, 2011 - July 28, 2011," in *Power and Energy Society General Meeting, 2011 IEEE*, ser. IEEE Power and Energy Society General Meeting. Pacific Northwest National Laboratory, Richland, WA 99354, United States: IEEE Computer Society, 2011, pp. 1–13. [Online]. Available: http://dx.doi.org/10.1109/PES.2011.6039913

[101] Y. V. Makarov, C. Loutan, J. Ma, and P. de Mello, "Operational Impacts of Wind Generation on California Power Systems," *Power Systems, IEEE Transactions on*, vol. 24, no. 2, pp. 1039–1050, 2009.

[102] A. Muzhikyan, A. M. Farid, and K. Youcef-Toumi, "An Enhanced Method for the Determination of Load Following Reserves," in *American Control Conference, 2014*, Portland, Oregon, 2014, pp. 1–8.

[103] P. S. Georgilakis, "Technical challenges associated with the integration of wind power into power systems," *Renewable and Sustainable Energy Reviews*, vol. 12, pp. 852–863, 2008.

[104] L. Soder and H. Holttinen, "On methodology for modelling wind power impact on power systems," *International Journal of Global Energy Issues*, vol. 29, no. 1-2, pp. 181–198, 2008.

[105] P. Kundur, *Power system stability and control.* McGraw-Hill, 1994.

[106] J. Machowski, J. W. Bialek, and J. R. Bumby, "Power system dynamics : stability and control," pp. xxvii, 629 p., 2008. [Online]. Available: http://www.loc.gov/catdir/toc/ecip0824/2008032220.html

[107] M. Eremia and M. Shahidehpour, *Handbook of electrical power system dynamics : modeling, stability, and control*, M. Eremia and M. Shahidehpour, Eds. Hoboken, N.J.: IEEE Press – John Wiley & Sons, 2013.

[108] F. Diaz-Gonzalez, M. Hau, A. Sumper, and O. Gomis-Bellmunt, "Participation of wind power plants in system frequency control : Review of grid code requirements and control methods," *Renewable and Sustainable Energy Reviews*, vol. 34, pp. 551–564, 2014.

[109] A. Muzhikyan, A. M. Farid, and K. Youcef-Toumi, "An Enterprise Control Assessment Method for Variable Energy Resource Induced Power System Imbalances Part 1: Methodology," *IEEE Transactions on Industrial Electronics (under revision)*, vol. X, no. X, pp. 1–9, 2014.

[110] ——, "A Power Grid Enterprise Control Method for Energy Storage System Integration," *IEEE Innovative Smart Grid Technologies Conference Europe*, pp. 1–6, 2014.

[111] ——, "Variable Energy Resource Induced Power System Imbalances: A Generalized Assessment Approach," Portland, Oregon, 2013, pp. 1–8. [Online]. Available: http://dx.doi.org.libproxy.mit.edu/10.1109/SusTech.2013.6617329

[112] ——, "Variable Energy Resource Induced Power System Imbalances: Mitigation by Increased System Flexibility, Spinning Reserves and Regulation," in *IEEE Conference on Technologies for Sustainability*, Portland, Oregon, 2013, pp. 1–7. [Online]. Available: http://dx.doi.org.libproxy.mit.edu/10.1109/SusTech.2013.6617292

[113] Y. T. Tan and D. S. Kirschen, "Co-optimization of Energy and Reserve in Electricity Markets with Demand-side Participation in Reserve Services," in *Power Systems Conference and Exposition, 2006. PSCE'06. 2006 IEEE PES*, October 2006, pp. 1182–1189.

[114] M. Ilic, L. Xie, and J.-Y. Joo, "Efficient Coordination of Wind Power and Price-Responsive Demand - Part I: Theoretical Foundations," *IEEE Transactions on Power Systems*, vol. 26, no. 4, pp. 1875–1884, November 2011.

[115] K. Dietrich, J. Latorre, L. Olmos, and A. Ramos, "Demand Response in an Isolated System With High Wind Integration," *IEEE Transactions on Power Systems*, vol. 27, no. 1, pp. 20–29, Feb 2012.

[116] S. Rahman and Rinaldy, "An efficient load model for analyzing demand side management impacts," *IEEE Transactions on Power Systems*, vol. 8, no. 3, pp. 1219–1226, Aug 1993.

[117] M. das Neves Queiroz de Macedo, J. J. M. Galo, L. A. L. Almeida, and A. C. C. Lima, "Opportunities and Challenges of DSM in Smart Grid Environment," *The Third International Conference on Smart Grids, Green Communications and IT Energy-aware Technologies*, pp. 156–160, 2013.

[118] D. Huang, R. Billinton, and W. Wangdee, "Effects of demand side management on bulk system adequacy evaluation," in *2010 IEEE 11th International Conference on Probabilistic Methods Applied to Power Systems (PMAPS)*, June 2010, pp. 593–598.

[119] S. Karnouskos, D. Ilic, and P. Silva, "Using flexible energy infrastructures for demand response in a Smart Grid city," in *2012 3rd IEEE PES International Conference and Exhibition on Innovative Smart Grid Technologies (ISGT Europe)*, Oct 2012, pp. 1–7.

[120] A. Rosso, J. Ma, D. S. Kirschen, and L. F. Ochoa, "Assessing the Contribution of Demand Side Management to Power System Flexibility," in *2011 50th IEEE Conference on Decision and Control and European Control Conference (CDC-ECC)*, 2011.

[121] S. Vandael, B. Claessens, M. Hommelberg, T. Holvoet, and G. Deconinck, "A Scalable Three-Step Approach for Demand Side Management of Plug-in Hybrid Vehicles," *IEEE Transactions on Smart Grid*, vol. 4, no. 2, pp. 720–728, June 2013.

[122] L. A. C. Lopes and M. Dalal-Bachi, "Economic Dispatch and Demand Side Management via Frequency Control in PV-Diesel Hybrid Mini-Grids," in *6th European Conference on PV-Hybrid and Mini-Grids, Chambery*, April 2012.

[123] P. Centolella, "The integration of Price Responsive Demand into Regional Transmission Organization (RTO) wholesale power markets and system operations," *Energy*, vol. 35, no. 4, pp. 1568 – 1574, 2010.

[124] L. A. Greening, "Demand response resources: Who is responsible for implementation in a deregulated market?" *Energy*, vol. 35, no. 4, pp. 1518 – 1525, 2010.

[125] Ontario Energy Board, "Demand-side Management and Demand Response in the Ontario Electricity Sector: Report of the Board to the Minister of Energy," Tech. Rep., Mar 2004.

[126] M. Fouda, Z. Fadlullah, N. Kato, A. Takeuchi, and Y. Nozaki, "A novel demand control policy for improving quality of power usage in smart grid," in *Global Communications Conference (GLOBECOM), 2012 IEEE*, Dec 2012, pp. 5154–5159.

[127] A.-H. Mohsenian-Rad, V. Wong, J. Jatskevich, R. Schober, and A. Leon-Garcia, "Autonomous Demand-Side Management Based on Game-Theoretic Energy Consumption Scheduling for the Future Smart Grid," *IEEE Transactions on Smart Grid*, vol. 1, no. 3, pp. 320–331, Dec 2010.

[128] I. Lampropoulos, P. van den Bosch, and W. Kling, "A predictive control scheme for automated demand response mechanisms," in *2012 3rd IEEE PES International Conference and Exhibition on Innovative Smart Grid Technologies (ISGT Europe)*, Oct 2012, pp. 1–8.

[129] B. Ramanathan and V. Vittal, "A Framework for Evaluation of Advanced Direct Load Control With Minimum Disruption," *IEEE Transactions on Power Systems*, vol. 23, no. 4, pp. 1681–1688, Nov 2008.

[130] Z. Fadlullah, D. M. Quan, N. Kato, and I. Stojmenovic, "GTES: An Optimized Game-Theoretic Demand-Side Management Scheme for Smart Grid," *IEEE Systems Journal*, vol. 8, no. 2, pp. 588–597, June 2014.

[131] Y. Liu, C. Yuen, S. Huang, N. Ul Hassan, X. Wang, and S. Xie, "Peak-to-Average Ratio Constrained Demand-Side Management With Consumer's Preference in Residential Smart Grid," *IEEE Journal of Selected Topics in Signal Processing*, vol. 8, no. 6, pp. 1084–1097, Dec 2014.

[132] Y. Tanoto, M. Santoso, and E. Hosea, "Multi-Dimensional Assessment for Residential Lighting Demand Side Management: A Proposed Framework," *Applied Mechanics and Materials*, vol. 284-287, pp. 3612–3616, 2013.

[133] S. Bahrami, M. Parniani, and A. Vafaeimehr, "A modified approach for residential load scheduling using smart meters," in *2012 3rd IEEE PES International Conference and Exhibition on Innovative Smart Grid Technologies (ISGT Europe)*, Oct 2012, pp. 1–8.

[134] M. Mazidi, A. Zakariazadeh, S. Jadid, and P. Siano, "Integrated scheduling of renewable generation and demand response programs in a microgrid," *Energy Conversion and Management*, vol. 86, pp. 1118–1127, 2014.

[135] K. Heussen, S. You, B. Biegel, L. Hansen, and K. Andersen, "Indirect control for demand side management - A conceptual introduction," in *2012 3rd IEEE PES International Conference and Exhibition on Innovative Smart Grid Technologies (ISGT Europe)*, Oct 2012, pp. 1–8.

[136] A. Molderink, V. Bakker, J. Hurink, and G. Smit, "Comparing demand side management approaches," in *2012 3rd IEEE PES International Conference and*

Exhibition on Innovative Smart Grid Technologies (ISGT Europe), Oct 2012, pp. 1–8.

[137] S. D. Ramchurn, P. Vytelingum, A. Rogers, and N. Jennings, "Agent-based control for decentralised demand side management in the smart grid," *The Tenth International Conference on Autonomous Agents and Multiagent Systems (AAMAS 2011)*, 2011.

[138] L. Wang, Z. Wang, and R. Yang, "Intelligent Multiagent Control System for Energy and Comfort Management in Smart and Sustainable Buildings," *IEEE Transactions on Smart Grid*, vol. 3, no. 2, pp. 605–617, June 2012.

[139] B. Claessens, S. Vandael, F. Ruelens, and M. Hommelberg, "Self-learning demand side management for a heterogeneous cluster of devices with binary control actions," in *2012 3rd IEEE PES International Conference and Exhibition on Innovative Smart Grid Technologies (ISGT Europe)*, Oct 2012, pp. 1–8.

[140] V. Muenzel, J. de Hoog, I. Mareels, A. Vishwanath, S. Kalyanaraman, and A. Gort, "PV Generation and Demand Mismatch: Evaluating the Potential of Residential Storage," *The IEEE PES Conference on Innovative Smart Grid Technologies 2015*, 2015.

[141] I. Atzeni, L. Ordonez, G. Scutari, D. Palomar, and J. Fonollosa, "Demand-Side Management via Distributed Energy Generation and Storage Optimization," *IEEE Transactions on Smart Grid*, vol. 4, no. 2, pp. 866–876, June 2013.

[142] N. Adilov, R. E. Schuler, W. D. Schulze, and D. E. Toomey, "The Effect of Customer Participation in Electricity Markets: An Experimental Analysis of Alternative Market Structures," in *The 37th Hawaii International Conference on System Sciences*, 2004.

[143] The Cadmus Group, Inc. / Energy Services, "Assessment of Long-Term, System-Wide Potential for Demand-Side and Other Supplemental Resources, 2013-2032 Volume I," March 2013.

[144] C. Goldman, N. Hopper, R. Bharvirkar, B. Neenan, and P. Cappers, "Estimating Demand Response Market Potential among Large Commercial and Industrial Customers: A Scoping Study," January 2007.

[145] A. B. Haney, T. Jamasb, L. M. Platchkov, and M. G. Pollitt, "Demand-side Management Strategies and the Residential Sector: Lessons from International Experience," November 2010.

[146] A. Muzhikyan, A. M. Farid, and K. Youcef-Toumi, "An Enterprise Control Assessment Method for Variable Energy Resource Induced Power System Imbalances Part 1: Methodology," *IEEE Transactions on Industrial Electronics*, vol. 62, no. 4, pp. 2448–2458, 2015. [Online]. Available: http://amfarid.scripts.mit.edu/resources/Journals/SPG-J15.pdf

[147] ——, "An Enterprise Control Assessment Method for Variable Energy Resource Induced Power System Imbalances Part 2: Results," *IEEE Transactions on Industrial Electronics*, vol. 62, no. 4, pp. 2459 – 2467, 2015. [Online]. Available: http://amfarid.scripts.mit.edu/resources/Journals/SPG-J16.pdf

[148] X. Zou, "Double-sided auction mechanism design in electricity based on maximizing social welfare," *Energy Policy*, vol. 37, no. 11, pp. 4231 – 4239, 2009.

[149] M. Govardhan and R. Roy, "Impact of demand side management on unit commitment problem," in *2014 International Conference on Control, Instrumentation, Energy and Communication (CIEC)*, Jan 2014, pp. 446–450.

[150] Y. Ikeda, T. Ikegami, K. Kataoka, and K. Ogimoto, "A Unit Commitment Model with Demand Response for the Integration of Renewable Energies," in *2012 IEEE Power and Energy Society General Meeting*, 2011.

[151] "Robust unit commitment problem with demand response and wind energy, author = Long Zhao and Bo Zeng," *2012 IEEE Power and Energy Society General Meeting*, pp. 1–8, 2012.

[152] H. Wu, M. Shahidehpour, and A. Al-Abdulwahab, "Hourly demand response in day-ahead scheduling for managing the variability of renewable energy," *IET Generation, Transmission & Distribution*, pp. 226–234, 2013.

[153] M. Kia, M. M. R. Sahebi, E. A. Duki, and S. H. Hosseini, "Simultaneous Implementation of Optimal Demand Response and Security Constrained Unit Commitment," in *2011 16th Conference on Electrical Power Distribution Networks (EPDC)*, 2011.

[154] J. Hurink, M. Bossman, A. Molderink, V. Bakker, and G. Smith, "Modeling, Simulation, and Optimization for the 21st Century Electric Power Grid," in *Engineering Conferences International*, 2012.

[155] F. Schneider, D. Klabjan, and U. W. Thonemann, "Incorporating Demand Response with Load Shifting into Stochastic Unit Commitment," April 2013.

[156] A. Gomez-Exposito, A. J. Conejo, and C. Canizares, *Electric Energy Systems: Analysis and Operation.* Boca Raton, FL: CRC Press, 2008.

[157] C. Harris, J. P. Meyers, and M. E. Webber, "A unit commitment study of the application of energy storage toward the integration of renewable generation," *Journal of Renewable and Sustainable Energy*, vol. 4, no. 1, p. 013120 (20 pp.), Jan 2012. [Online]. Available: http://dx.doi.org/10.1063/1.3683529

[158] B. F. Hobbs, M. H. Rothkopf, R. P. ONeill, and H.-p. Chao, *The Next Generation of Electric Power Unit Commitment Models.* New York, NY, USA: Kluwer Academic Publishers, 2001.

[159] M. Nazari, M. Ardehali, and S. Jafari, "Pumped-storage unit commitment with considerations for energy demand, economics, and environmental constraints," *Energy*, vol. 35, no. 10, pp. 4092–4101, Oct 2010.

[160] T. Senjyu, T. Miyagi, S. A. Yousuf, N. Urasaki, and T. Funabashi, "A technique for unit commitment with energy storage system," *International Journal of Electrical Power & Energy Systems*, vol. 29, no. 1, pp. 91–98, Jan 2007. [Online]. Available: http://dx.doi.org/10.1016/j.ijepes.2006.05.004

[161] L. Wu, M. Shahidehpour, and T. Li, "Stochastic security-constrained unit commitment," *IEEE Trans. Power Syst.*, vol. 22, no. 2, pp. 800–811, May 2007.

[162] T. J. Brennan, "Demand-Side Management Programs Under Retail Electricity Competition," 1998.

[163] B. Jiang, A. Farid, and K. Youcef-Toumi, "A Comparison of Day-Ahead Wholesale Market: Social Welfare vs Industrial Demand Side Management," in *2015 IEEE International Conference on Industrial Technology*, March 2015.

[164] Y. Fu, M. Shahidehpour, and Z. Li, "Security-constrained unit commitment with ac constraints," *IEEE Transactions on Power Systems*, vol. 20, no. 2, pp. 1001–1013, 2005.

[165] BPA, "Data for BPA Balancing Authority Total Load, Wind Gen, Wind Forecast, Hydro, Thermal, and Net Interchange," 2014. [Online]. Available: http://transmission.bpa.gov/business/operations/wind/

[166] A. Muzhikyan, A. Farid, and K. Youcef-Toumi, "Variable Energy Resource Induced Power System Imbalances: A Generalized Assessment Approach," in *2013 1st IEEE Conference on Technologies for Sustainability (SusTech)*, 2013, pp. 1–8.

[167] A. Muzhikyan, A. M. Farid, and K. Youcef-Toumi, "Variable Energy Resource Induced Power System Imbalances: Mitigation by Increased System Flexibility, Spinning Reserves and Regulation," in *2013 1st IEEE Conference on Technologies for Sustainability (SusTech)*, Aug 2013, pp. 15–22.

[168] H. Holttinen, M. Milligan, E. Ela, N. Menemenlis, J. Dobschinski, B. Rawn, R. J. Bessa, D. Flynn, E. Gomez-Lazaro, and N. K. Detlefsen, "Methodologies to Determine Operating Reserves Due to Increased Wind Power," *Sustainable Energy, IEEE Transactions on*, vol. 3, no. 4, pp. 713–723, 2012.

[169] K.-S. Kim, L.-H. Jung, S.-C. Lee, and U.-C. Moon, "Security Constrained Economic Dispatch Using Interior Point Method," in *Power System Technology, 2006. PowerCon 2006. International Conference on*, 2006, pp. 1–6.

[170] L. S. Vargas, V. H. Quintana, and A. Vannelli, "A Tutorial Description of an Interior Point Method and Its Applications to Security-Constrained Economic

Dispatch," *Power Systems, IEEE Transactions on*, vol. 8, no. 3, pp. 1315–1324, 1993.

[171] C. Grigg, P. Wong, P. Albrecht, R. Allan, M. Bhavaraju, R. Billinton, Q. Chen, C. Fong, S. Haddad, S. Kuruganty, W. Li, R. Mukerji, D. Patton, N. Rau, D. Reppen, A. Schneider, M. Shahidehpour, and C. Singh, "The IEEE Reliability Test System-1996. A report prepared by the Reliability Test System Task Force of the Application of Probability Methods Subcommittee," *Power Systems, IEEE Transactions on*, vol. 14, no. 3, pp. 1010–1020, 1999.

[172] A. V. Oppenheim and R. W. Schafer, *Discrete-Time Signal Processing*, 3rd ed. Prentice Hall, 2010.

[173] P. Sorensen and N. A. Cutululis, "Wind farms' spatial distribution effect on power system reserves requirements," in *Industrial Electronics (ISIE), 2010 IEEE International Symposium on*, 2010, pp. 2505–2510.

[174] A. Farid and A. Muzhikyan, "The Need for Holistic Assessment Methods for the Future Electricity Grid," in *GCC CIGRE Power*, 2013, pp. 1–12.

Appendix A

Figures

Contents

clean up

```
close all; clear all; clc;
tic
```

use both methods and compare the results

```
% SW approach
mpc = testcase;
exportSCUC_SW(mpc);
gams('commitment_SW_new.gms');
mpc = importSCUC_SW(mpc);
% mainplot_SW(mpc)
save('SW_120','mpc')

% PJM approach
mpc = testcase;
exportSCUC_PJM(mpc);
gams('commitment_PJM_new.gms');
mpc = importSCUC_PJM(mpc);
% mainplot_PJM(mpc)
save('PJM_120','mpc')

% plot and compare results
mainplot

toc
```

Published with MATLAB® R2014b

Figure A-1: Top Level File MATLAB

Contents


```
function exportSCUC_SW(mpc)
```

```
% system parameters
T.name  = 't';
T.type  = 'set';
T.val   = mpc.Nh';

NetLoad.name    = 'NetLoad';
NetLoad.type   = 'parameter';
NetLoad.form    = 'sparse';
NetLoad.val     = [ mpc.Nh', mpc.sw_net' ];
```

dispatchable generator

```
I.name  = 'i';
I.type  = 'set';
I.val   = mpc.gc.ind';

GCPmax.name     = 'GCPmax';
GCPmax.type     = 'parameter';
GCPmax.form     = 'sparse';
GCPmax.val      = [ mpc.gc.ind', mpc.gc.pmax' ];

GCPmin.name     = 'GCPmin';
GCPmin.type     = 'parameter';
GCPmin.form     = 'sparse';
GCPmin.val      = [ mpc.gc.ind', mpc.gc.pmin' ];

GCRmax.name     = 'GCRmax';
GCRmax.type     = 'parameter';
GCRmax.form     = 'sparse';
GCRmax.val      = [ mpc.gc.ind', mpc.gc.rmax' ];

GCRmin.name     = 'GCRmin';
GCRmin.type     = 'parameter';
GCRmin.form     = 'sparse';
GCRmin.val      = [ mpc.gc.ind', mpc.gc.rmin' ];

GCzeta.name     = 'GCzeta';
GCzeta.type     = 'parameter';
GCzeta.form     = 'sparse';
GCzeta.val      = [ mpc.gc.ind', mpc.gc.zeta' ];

GCB.name     = 'GCB';
GCB.type     = 'parameter';
```

```
GCB.form     = 'sparse';
GCB.val      = [ mpc.gc.ind', mpc.gc.b' ];

GCA.name     = 'GCA';
GCA.type     = 'parameter';
GCA.form     = 'sparse';
GCA.val      = [ mpc.gc.ind', mpc.gc.a' ];

GCS.name     = 'GCS';
GCS.type     = 'parameter';
GCS.form     = 'sparse';
GCS.val      = [ mpc.gc.ind', mpc.gc.s' ];

GCD.name     = 'GCD';
GCD.type     = 'parameter';
GCD.form     = 'sparse';
GCD.val      = [ mpc.gc.ind', mpc.gc.d' ];
```

DC parameters

```
J.name  = 'j';
J.type  = 'set';
J.val   = mpc.dc.ind';

DCPmax.name     = 'DCPmax';
DCPmax.type     = 'parameter';
DCPmax.form     = 'sparse';
DCPmax.val      = [ mpc.dc.ind', mpc.dc.pmax' ];

DCPmin.name     = 'DCPmin';
DCPmin.type     = 'parameter';
DCPmin.form     = 'sparse';
DCPmin.val      = [ mpc.dc.ind', mpc.dc.pmin' ];

DCPbase.name    = 'DCPbase';
DCPbase.type    = 'parameter';
DCPbase.form    = 'sparse';
DCPbase.val     = [mpc.dc.ind', mpc.dc.baseline' ];

DCRmax.name     = 'DCRmax';
DCRmax.type     = 'parameter';
DCRmax.form     = 'sparse';
DCRmax.val      = [ mpc.dc.ind', mpc.dc.rmax' ];

DCRmin.name     = 'DCRmin';
DCRmin.type     = 'parameter';
DCRmin.form     = 'sparse';
DCRmin.val      = [ mpc.dc.ind', mpc.dc.rmin' ];

DCzeta.name     = 'DCzeta';
DCzeta.type     = 'parameter';
DCzeta.form     = 'sparse';
DCzeta.val      = [ mpc.dc.ind', mpc.dc.zeta' ];

DCB.name     = 'DCB';
DCB.type     = 'parameter';
```

```
DCB.form      = 'sparse';
DCB.val       = [ mpc.dc.ind', mpc.dc.b' ];

DCA.name      = 'DCA';
DCA.type      = 'parameter';
DCA.form      = 'sparse';
DCA.val       = [ mpc.dc.ind', mpc.dc.a' ];

DCS.name      = 'DCS';
DCS.type      = 'parameter';
DCS.form      = 'sparse';
DCS.val       = [ mpc.dc.ind', mpc.dc.s' ];

DCD.name      = 'DCD';
DCD.type      = 'parameter';
DCD.form      = 'sparse';
DCD.val       = [ mpc.dc.ind', mpc.dc.d' ];
```

export data to GAMS

```
wgdx('UC-Data-SW', T, I, NetLoad, GCPmax, GCPmin, GCRmax, GCRmin, GCzeta, GCB, GCA, GCS, GCD,...
    J, DCPmax, DCPmin, DCPbase, DCRmax, DCRmin, DCB, DCA);
```

Published with MATLAB® R2014b

```
sets
        i       GC indices,
        j       DC indices
        t       time interval indices;

parameters
        NetLoad(t)      SW stochastic netload,

        GCPmax(i),
        GCPmin(i),
        GCRmax(i),
        GCRmin(i),
        GCzeta(i),
        GCB(i),
        GCA(i),
        GCS(i),
        GCD(i),

        DCPmax(j),
        DCPmin(j),
        DCPbase(j),
        DCRmax(j),
        DCRmin(j),
        DCB(j),
        DCA(j);

$gdxin UC-Data-SW
$load i j t NetLoad GCPmax GCPmin GCRmax GCRmin GCzeta GCB GCA GCS GCD DCPmax DC»
Pmin DCPbase DCRmax DCRmin DCB DCA
$gdxin

Parameter pPGC(i,t);
Parameter pRGC(i,t);
Parameter psumPGC(t);
Parameter pwGC(i,t);
Parameter pwUGC(i,t);
Parameter pwDGC(i,t);

Parameter pPDC(j,t);
Parameter pRDC(j,t);
Parameter psumPDC(t);
Parameter pwDC(j,t);
Parameter pwUDC(j,t);
Parameter pwDDC(j,t);


free variable
        z                       object function,
        vGC,
        vGCs,
        vGCr,
        vDC,

        RGC(i,t),
        RDC(j,t);

positive variable
        PGC(i,t),
        PDC(j,t);
```

```
binary variables
        wGC(i,t),
        wUGC(i,t),
        wDGC(i,t),

        wDC(j,t),
        wUDC(j,t),
        wDDC(j,t);

equations
        eCost,
        eGC,
        eGCs,
        eGCr,
        eDC,

        eBalance(t),

        eGCPmax(i,t),
        eGCPmin(i,t),
        eGCRamp(i,t),
        eGCRmax(i,t),
        eGCRmin(i,t),
        eGCStates(i,t),

        eDCPmax(j,t),
        eDCPmin(j,t),
        eDCRamp(j,t),
        eDCRmax(j,t),
        eDCRmin(j,t),
        eDCStates(j,t);

eCost..                 z    =e= vGC - vDC;
eGC..                   vGC  =e= vGCs + vGCr + 0.001*sum((i,t),wUGC(i,t) + wDGC(i,t));
eGCs..                  vGCs =e= sum( (i,t), wUGC(i,t)*GCS(i) );
eGCr..                  vGCr =e= sum( (i,t), wGC(i,t)*GCzeta(i) + GCB(i)*PGC(i,t) + GCA(i)*PGC(i,t)*PGC(i,t) );
eDC..                   vDC  =e= sum( (j,t), DCB(j)*PDC(j,t) + DCA(j)*PDC(j,t)*PDC(j,t) );

eBalance(t)..           sum(i, PGC(i,t)) =e= NetLoad(t) + sum(j, PDC(j,t));

eGCPmax(i,t)..          PGC(i,t) =l= wGC(i,t)*GCPmax(i);
eGCPmin(i,t)..          PGC(i,t) =g= wGC(i,t)*GCPmin(i);
eGCRamp(i,t)..          RGC(i,t) =e= PGC(i,t) - PGC(i,t--1);
eGCRmax(i,t)..          RGC(i,t) =l= GCRmax(i);
eGCRmin(i,t)..          RGC(i,t) =g= GCRmin(i);
eGCStates(i,t)..        wGC(i,t) =e= wGC(i,t--1) + wUGC(i,t) - wDGC(i,t);

eDCPmax(j,t)..          PDC(j,t) =l= wDC(j,t)*DCPmax(j);
eDCPmin(j,t)..          PDC(j,t) =g= wDC(j,t)*DCPmin(j);
eDCRamp(j,t)..          RDC(j,t) =e= PDC(j,t) - PDC(j,t--1);
eDCRmax(j,t)..          RDC(j,t) =l= DCRmax(j);
eDCRmin(j,t)..          RDC(j,t) =g= DCRmin(j);
eDCStates(j,t)..        wDC(j,t) =e= wDC(j,t--1) + wUDC(j,t) - wDDC(j,t);


option MIQCP = cplex;

```

```
model commitment /all/;
*commitment.optCR = 0.001;
commitment.optCR = 0.0000000001;
solve commitment using miqcp minimizing z;

pPGC(i,t)         = PGC.l(i,t);
pRGC(i,t)         = RGC.l(i,t);
psumPGC(t)        = sum(i, PGC.l(i,t));
pwGC(i,t)         = wGC.l(i,t);
pwUGC(i,t)        = wUGC.l(i,t);
pwDGC(i,t)        = wDGC.l(i,t);

pPDC(j,t)         = PDC.l(j,t);
pRDC(j,t)         = RDC.l(j,t);
psumPDC(t)        = sum(j, PDC.l(j,t));
pwDC(j,t)         = wDC.l(j,t);
pwUDC(j,t)        = wUDC.l(j,t);
pwDDC(j,t)        = wDDC.l(j,t);

execute_unload 'UC-Sol-SW', pPGC, pRGC, psumPGC, pwGC, pwUGC, pwDGC, pPDC, pRDC,»
    psumPDC, pwDC, pwUDC, pwDDC;
```

```
function mpc = importSCUC_SW(mpc)

% read GC results
pPGC    = rgdx('UC-Sol-SW', struct('name', 'pPGC',  'form', 'full'));
pRGC    = rgdx('UC-Sol-SW', struct('name', 'pRGC',  'form', 'full'));
pwGC    = rgdx('UC-Sol-SW', struct('name', 'pwGC',  'form', 'full'));
pwUGC   = rgdx('UC-Sol-SW', struct('name', 'pwUGC', 'form', 'full'));
% pwDGC   = rgdx('UC-Sol-SW', struct('name', 'pwDGC', 'form', 'full'));

mpc.GCresults.PGC   = pPGC.val(mpc.gc.ind, mpc.Nh);
mpc.GCresults.RGC   = pRGC.val(mpc.gc.ind, mpc.Nh);
mpc.GCresults.wGC   = pwGC.val(mpc.gc.ind, mpc.Nh);
mpc.GCresults.wUGC  = pwUGC.val(mpc.gc.ind, mpc.Nh);
% mpc.GCresults.wDGC  = pwDGC.val(mpc.gc.ind, mpc.Nh);


% read DC results
pPDC    = rgdx('UC-Sol-SW', struct('name', 'pPDC',  'form', 'full'));
pRDC    = rgdx('UC-Sol-SW', struct('name', 'pRDC',  'form', 'full'));
pwDC    = rgdx('UC-Sol-SW', struct('name', 'pwDC',  'form', 'full'));
% pwUDC   = rgdx('UC-Sol-SW', struct('name', 'pwUDC', 'form', 'full'));
% pwDDC   = rgdx('UC-Sol-SW', struct('name', 'pwDDC', 'form', 'full'));

mpc.DCresults.PDC   = pPDC.val(mpc.dc.ind, mpc.Nh);
mpc.DCresults.RDC   = pRDC.val(mpc.dc.ind, mpc.Nh);
mpc.DCresults.wDC   = pwDC.val(mpc.dc.ind, mpc.Nh);
% mpc.DCresults.wUDC  = pwUDC.val(mpc.dc.ind, mpc.Nh);
% mpc.DCresults.wDDC  = pwDDC.val(mpc.dc.ind, mpc.Nh);

end
```

Published with MATLAB® R2014b

Figure A-2: Social Welfare DSM Model MATLAB

Contents


```
function exportSCUC_PJM(mpc)
```

```
% system parameters
T.name  = 't';
T.type  = 'set';
T.val   = mpc.Nh';

NetLoad.name    = 'NetLoad';
NetLoad.type   = 'parameter';
NetLoad.form    = 'sparse';
NetLoad.val     = [ mpc.Nh', mpc.pjm_net' ];
```

dispatchable generator

```
I.name  = 'i';
I.type  = 'set';
I.val   = mpc.gc.ind';

GCPmax.name     = 'GCPmax';
GCPmax.type     = 'parameter';
GCPmax.form     = 'sparse';
GCPmax.val      = [ mpc.gc.ind', mpc.gc.pmax' ];

GCPmin.name     = 'GCPmin';
GCPmin.type     = 'parameter';
GCPmin.form     = 'sparse';
GCPmin.val      = [ mpc.gc.ind', mpc.gc.pmin' ];

GCRmax.name     = 'GCRmax';
GCRmax.type     = 'parameter';
GCRmax.form     = 'sparse';
GCRmax.val      = [ mpc.gc.ind', mpc.gc.rmax' ];

GCRmin.name     = 'GCRmin';
GCRmin.type     = 'parameter';
GCRmin.form     = 'sparse';
GCRmin.val      = [ mpc.gc.ind', mpc.gc.rmin' ];

GCzeta.name     = 'GCzeta';
GCzeta.type     = 'parameter';
GCzeta.form     = 'sparse';
GCzeta.val      = [ mpc.gc.ind', mpc.gc.zeta' ];

GCB.name     = 'GCB';
GCB.type     = 'parameter';
```

```
GCB.form     = 'sparse';
GCB.val      = [ mpc.gc.ind', mpc.gc.b' ];

GCA.name     = 'GCA';
GCA.type     = 'parameter';
GCA.form     = 'sparse';
GCA.val      = [ mpc.gc.ind', mpc.gc.a' ];

GCS.name     = 'GCS';
GCS.type     = 'parameter';
GCS.form     = 'sparse';
GCS.val      = [ mpc.gc.ind', mpc.gc.s' ];

GCD.name     = 'GCD';
GCD.type     = 'parameter';
GCD.form     = 'sparse';
GCD.val      = [ mpc.gc.ind', mpc.gc.d' ];
```

DC parameters

```
J.name  = 'j';
J.type  = 'set';
J.val   = mpc.dc.ind';

GVPmax.name     = 'GVPmax';
GVPmax.type     = 'parameter';
GVPmax.form     = 'sparse';
GVPmax.val      = [ mpc.dc.ind', mpc.dc.baseline' ];

GVPmin.name     = 'GVPmin';
GVPmin.type     = 'parameter';
GVPmin.form     = 'sparse';
% GVPmin.val      = [ mpc.dc.ind', mpc.dc.baseline' - mpc.dc.pmax' ];
GVPmin.val      = [mpc.dc.ind', mpc.dc.pmin'];

GVPbase.name    = 'GVPbase';
GVPbase.type    = 'parameter';
GVPbase.form    = 'sparse';
GVPbase.val     = [mpc.dc.ind', mpc.dc.baseline' ];

GVRmax.name     = 'GVRmax';
GVRmax.type     = 'parameter';
GVRmax.form     = 'sparse';
GVRmax.val      = [ mpc.dc.ind', mpc.dc.rmax' ];

GVRmin.name     = 'GVRmin';
GVRmin.type     = 'parameter';
GVRmin.form     = 'sparse';
GVRmin.val      = [ mpc.dc.ind', mpc.dc.rmin' ];

GVzeta.name     = 'GVzeta';
GVzeta.type     = 'parameter';
GVzeta.form     = 'sparse';
GVzeta.val      = [ mpc.dc.ind', mpc.dc.zeta' ];

GVB.name     = 'GVB';
```

```
GVB.type     = 'parameter';
GVB.form     = 'sparse';
% calculate the PJM DC coeff. from the SW coeff.
GVB.val      = [ mpc.dc.ind', mpc.gv.b'];

GVA.name     = 'GVA';
GVA.type     = 'parameter';
GVA.form     = 'sparse';
% calculate the PJM DC coeff. from the SW coeff.
GVA.val      = [ mpc.dc.ind', mpc.gv.a' ];

GVS.name     = 'GVS';
GVS.type     = 'parameter';
GVS.form     = 'sparse';
GVS.val      = [ mpc.dc.ind', mpc.dc.s' ];

GVD.name     = 'GVD';
GVD.type     = 'parameter';
GVD.form     = 'sparse';
GVD.val      = [ mpc.dc.ind', mpc.dc.d' ];
```

export data to GAMS

```
wgdx('UC-Data-PJM', T, I, NetLoad, GCPmax, GCPmin, GCRmax, GCRmin, GCzeta, GCB, GCA, GCS, GCD,...
    J, GVPmax, GVPmin, GVPbase, GVRmax, GVRmin, GVB, GVA);
```

```
end
```

Published with MATLAB® R2014b

```
sets
        i       GC indices,
        j       DC indices
        t       time interval indices;

parameters
        NetLoad(t)      SW stochastic netload,

        GCPmax(i),
        GCPmin(i),
        GCRmax(i),
        GCRmin(i),
        GCzeta(i),
        GCB(i),
        GCA(i),
        GCS(i),
        GCD(i),

        GVPmax(j),
        GVPmin(j),
        GVPbase(j),
        GVRmax(j),
        GVRmin(j),
        GVB(j),
        GVA(j);

$gdxin UC-Data-PJM
$load i j t NetLoad GCPmax GCPmin GCRmax GCRmin GCzeta GCB GCA GCS GCD GVPmax GV»
Pmin GVPbase GVRmax GVRmin GVB GVA
$gdxin

Parameter pPGC(i,t);
Parameter pRGC(i,t);
Parameter psumPGC(t);
Parameter pwGC(i,t);
Parameter pwUGC(i,t);
Parameter pwDGC(i,t);

Parameter pPGV(j,t);
Parameter pRGV(j,t);
Parameter psumPGV(t);
Parameter pwGV(j,t);
Parameter pwUGV(j,t);
Parameter pwDGV(j,t);
Parameter pz;


free variable
        z                       object function,
        vGC,
        vGCs,
        vGCr,
        vGV,

        RGC(i,t),
        RGV(j,t);

positive variable
        PGC(i,t),
        PGV(j,t);
```

```
60
61 binary variables
62          wGC(i,t),
63          wUGC(i,t),
64          wDGC(i,t),
65
66          wGV(j,t),
67          wUGV(j,t),
68          wDGV(j,t);
69
70 equations
71          eCost,
72          eGC,
73          eGCs,
74          eGCr,
75          eGV,
76
77          eBalance(t),
78
79          eGCPmax(i,t),
80          eGCPmin(i,t),
81          eGCRamp(i,t),
82          eGCRmax(i,t),
83          eGCRmin(i,t),
84          eGCStates(i,t),
85
86          eGVPmax(j,t),
87          eGVPmin(j,t),
88          eGVRamp(j,t),
89          eGVRmax(j,t),
90          eGVRmin(j,t),
91          eGVStates(j,t);
92
93 eCost..                    z    =e= vGC + vGV;
94 eGC..                      vGC  =e= vGCs + vGCr + 0.001*sum((i,t),wUGC(i,t) + wDGC»
   (i,t));
95 eGCs..                     vGCs =e= sum( (i,t), wUGC(i,t)*GCS(i) );
96 eGCr..                     vGCr =e= sum( (i,t), wGC(i,t)*GCzeta(i) + GCB(i)*PGC(i,»
   t) + GCA(i)*PGC(i,t)*PGC(i,t) );
97 eGV..                      vGV  =e= sum( (j,t), GVB(j)*PGV(j,t) + GVA(j)*PGV(j,t)*»
   PGV(j,t) );
98
99 eBalance(t)..              sum(i, PGC(i,t)) + sum(j, PGV(j,t)) =e= NetLoad(t);
100
101 eGCPmax(i,t)..            PGC(i,t) =l= wGC(i,t)*GCPmax(i);
102 eGCPmin(i,t)..            PGC(i,t) =g= wGC(i,t)*GCPmin(i);
103 eGCRamp(i,t)..            RGC(i,t) =e= PGC(i,t) - PGC(i,t--1);
104 eGCRmax(i,t)..            RGC(i,t) =l= GCRmax(i);
105 eGCRmin(i,t)..            RGC(i,t) =g= GCRmin(i);
106 eGCStates(i,t)..          wGC(i,t) =e= wGC(i,t--1) + wUGC(i,t) - wDGC(i,t);
107
108 eGVPmax(j,t)..            PGV(j,t) =l= wGV(j,t)*GVPmax(j);
109 eGVPmin(j,t)..            PGV(j,t) =g= wGV(j,t)*GVPmin(j);
110 eGVRamp(j,t)..            RGV(j,t) =e= PGV(j,t) - PGV(j,t--1);
111 eGVRmax(j,t)..            RGV(j,t) =l= GVRmax(j);
112 eGVRmin(j,t)..            RGV(j,t) =g= GVRmin(j);
113 eGVStates(j,t)..          wGV(j,t) =e= wGV(j,t--1) + wUGV(j,t) - wDGV(j,t);
114
115 option MIQCP = cplex;
116 OPTION ITERLIM = 10000000;
```

```
model commitment /all/;
commitment.optCR = 0.0000000001;
solve commitment using miqcp minimizing z;

pPGC(i,t)         = PGC.l(i,t);
pRGC(i,t)         = RGC.l(i,t);
psumPGC(t)        = sum(i, PGC.l(i,t));
pwGC(i,t)         = wGC.l(i,t);
pwUGC(i,t)        = wUGC.l(i,t);
pwDGC(i,t)        = wDGC.l(i,t);

pPGV(j,t)         = PGV.l(j,t);
pRGV(j,t)         = RGV.l(j,t);
psumPGV(t)        = sum(j, PGV.l(j,t));
pwGV(j,t)         = wGV.l(j,t);
pwUGV(j,t)        = wUGV.l(j,t);
pwDGV(j,t)        = wDGV.l(j,t);
pz                = z.l;


execute_unload 'UC-Sol-PJM', pPGC, pRGC, psumPGC, pwGC, pwUGC, pwDGC, pPGV, pRGV»
, psumPGV, pwGV, pwUGV, pwDGV, pz;
```

```
function mpc = importSCUC_PJM(mpc)

% read GC results
pPGC    = rgdx('UC-Sol-PJM', struct('name', 'pPGC',  'form', 'full'));
pRGC    = rgdx('UC-Sol-PJM', struct('name', 'pRGC',  'form', 'full'));
pwGC    = rgdx('UC-Sol-PJM', struct('name', 'pwGC',  'form', 'full'));
pwUGC   = rgdx('UC-Sol-PJM', struct('name', 'pwUGC', 'form', 'full'));
pwDGC   = rgdx('UC-Sol-PJM', struct('name', 'pwDGC', 'form', 'full'));

mpc.GCresults.PGC   = pPGC.val(mpc.gc.ind, mpc.Nh);
mpc.GCresults.RGC   = pRGC.val(mpc.gc.ind, mpc.Nh);
mpc.GCresults.wGC   = pwGC.val(mpc.gc.ind, mpc.Nh);
mpc.GCresults.wUGC  = pwUGC.val(mpc.gc.ind, mpc.Nh);
mpc.GCresults.wDGC  = pwDGC.val(mpc.gc.ind, mpc.Nh);


% read DC results
pPGV    = rgdx('UC-Sol-PJM', struct('name', 'pPGV',  'form', 'full'));
pRGV    = rgdx('UC-Sol-PJM', struct('name', 'pRGV',  'form', 'full'));
pwGV    = rgdx('UC-Sol-PJM', struct('name', 'pwGV',  'form', 'full'));
% pwUGV   = rgdx('UC-Sol-PJM', struct('name', 'pwUGV', 'form', 'full'));
% pwDGV   = rgdx('UC-Sol-PJM', struct('name', 'pwDGV', 'form', 'full'));

mpc.GVresults.PGV   = pPGV.val(mpc.dc.ind, mpc.Nh);
mpc.GVresults.RGV   = pRGV.val(mpc.dc.ind, mpc.Nh);
mpc.GVresults.wGV   = pwGV.val(mpc.dc.ind, mpc.Nh);
% mpc.GVresults.wUGV  = pwUGV.val(mpc.dc.ind, mpc.Nh);
% mpc.GVresults.wDGV  = pwDGV.val(mpc.dc.ind, mpc.Nh);

pz          = rgdx('UC-Sol-PJM', struct('name', 'pz', 'form', 'full'));
mpc.pjmz    = pz.val(1,1);

end
```

Published with MATLAB® R2014b

Figure A-3: Industrial DSM Model MATLAB